Reservoir and Source Potential of Eocene Microbialites, Green River Formation, USA

by

Nicholas Cestari

Submitted to the Department of Geology
and the Faculty of the Graduate School of the University of Kansas in
partial fulfillment of the requirements for the
degree of Master of Science.

Advisory Committee:

_____
Alison Olcott Marshall, Chair

_____
Craig P. Marshall

_____
Eugene C. Rankey

Date Defended: 12/2/2015

The Thesis Committee for Nicholas Cestari
certifies that this is the approved version of the following thesis:

Reservoir and Source Potential of Eocene Microbialites, Green River Formation, USA

_____
Alison Olcott Marshall, Ph.D., Chairperson

Date Approved: 12/2/2015

ABSTRACT

In recent years, large petroleum discoveries within the lacustrine microbialite facies of pre-salt systems of offshore Brazil, Angola, and Gabon have increased interest in the potential of microbial carbonates as reservoir rocks. Whereas a multitude of studies have been conducted on microbialites and the associated lacustrine facies separately, there is still little known regarding whether there are definitive dissimilarities between the geochemical footprints of microbialites and associated lithofacies within a system. To explore this unknown, organic geochemistry was evaluated with the aim of comparing the microbialite facies (stromatolites and thrombolites) with the associated lacustrine carbonates (dolomitic marlstone, ooid grainstone, peloidal packstone and wackestone) to test if there are dissimilarities in regard to reservoir and source potential. Specifically, the goal is to understand the petroleum significance of lacustrine microbialites deposited in various lake conditions.

Total Organic Carbon (TOC) and extractable organic material were analyzed for microbialite and associated lacustrine lithofacies in the Green River Formation of Colorado and Utah. The samples were from three cores: two from Piceance Basin (Nielsen 17-1 and Colorado Core 01A) and one from Uinta Basin (1 Coyote Wash). Additional hand samples collected from an outcrop at Douglas Pass, Colorado, represent shallow lake-margin deposits.

The lake of the Piceance Creek Basin was a hydrologically closed, hypersaline lake characterized by deposition of organic rich microbialites, and dolomitic marlstones. In contrast, the Uinta Basin lake was a hydrologically open lake characterized by accumulation of organically lean microbialites, siltstone, mudstone, ooid grainstone, and

peloidal packstone and wackestone. Gas chromatography/mass spectroscopy (GC/MS) analysis yielded biomarker distributions distinct between the lacustrine microbialite facies and the associated lithofacies. The abundance of biomarkers associated with hydrocarbon potential is 10 to 100x greater in the microbialites than in the associated lacustrine carbonate lithofacies. Understanding the geochemical footprints of lacustrine microbialites and how they differ from associated carbonates as a function of depositional environment is crucial in identifying prospects in similar ancient reservoir systems.

Acknowledgements

I would like to thank the University of Kansas for the opportunity to complete my Masters degree. However, if it weren't for Alison Olcott Marshall I would never have had this opportunity to grow in my scientific background. I truly appreciate everything that she has sacrificed to make sure I completed everything to the best of my ability and in a timely manner. Alison was a great mentor to me throughout the whole process never letting me get discouraged and always causing me to reach farther in my brain for an answer. I have learned so much and gained valuable expertise that will help better my future in oil and gas. My committee members Craig Marshall and Gene Rankey provided valuable feedback that helped me reach my goal. I was challenged in ways that bettered me as a student and person throughout this journey. I couldn't have done it without the help of the USGS Core Research Center in Denver Colorado with sampling core for my research. Dr. Rick Sarg was of great assistance with guiding me to the outcrop of Douglas Pass so that I was able to do field work and collect my samples for analysis. I want to also extend a great deal of gratitude to the fellow graduate students in my lab Brenden Keel and Ted Morehouse who were a source of constant support and relief. I couldn't have done this without the constant encouragement coming from my family that truly got me through some of my toughest days. I owe a great deal to all of those who supported, and guided me throughout this learning process.

TABLE OF CONTENTS

CHAPTER ONE

1.1 Introduction

In recent years, reserves of oil and gas have been discovered in basins off the coast of Brazil, Angola, and Gabon in the Cretaceous layers known as the "pre-salt." The main reservoirs in the Brazilian "pre-salt" correspond to stromatolitic and bioclastic carbonate facies deposited in lacustrine to shallow marine depositional environments during the "sag" phase (Hamon et al., 2013). Since there is limited subsurface data for interpreting the pre-salt system, the reservoir distribution and reservoir heterogeneities are poorly understood for the lacustrine to shallow marine sag phase. Thus, the search for suitable modern analogs to the large lacustrine microbial carbonate reservoirs has been ongoing, yet no system matches the spatial extent of the "pre-salt" reservoirs. However, some ancient depositional analogs to the "pre-salt" include outstanding outcrop exposures and have been cored and analyzed. The most prominent of these analogs are the Eocene Green River Formation of the western U.S. and the late Archean Meentheena Member of the Tumbiana Formation of Western Australia (Awramik and Buchheim, 2012). The microbialites for the Meentheena Member are diverse; stromatolites dominate, and are laterally extensive for tens of kilometers, whereas in the Green River Formation stromatolites are much less extensive, but are much thicker (Awramik and Buchheim, 2012). These microbialite deposits in the Meentheena Member and Green River formation have garnered so much attention as possible analogs to the "pre-salt" in sections of offshore Santos Basin, Brazil, where microbialites and associated lacustrine facies are reported to form significant reservoirs (Buchheim, et al., 2012). There is even a

stromatolitic mound reservoir in the Eocene Green River Formation in Utah (Osmond et al., 2000). Beyond general depositional facies, in the past few years, numerous studies have investigated the spatial relationships of microbialites in outcrop, or on porosity-permeability relationships within microbialites (Awramik and Buchheim, 2012; Bohacs et al., 2013; George et al., 2012; Al Haddad and Mancini, 2013; Hamon et al., 2012; Kopaska-Merkel et al., 2013; Mancini and Parcell, 2001; Osburn et al., 2013; Sarg et al., 2013; Seard, et., 2013; Slowakiewicz et al., 2013; Wahlman et al., 2013; Warusavitharana and Parcell, 2013). In spite of the numerous studies, only one (Slowakiewicz et al., 2013) involved organic geochemistry, and it was used only to determine the thermal maturity of the rocks. To date, no study has analyzed the organic matter preserved in microbialites and compared it directly with the surrounding lithofacies (mudstone, dolomitic marlstone, oolitic grainstone, peloidal wackestones/packstones) to provide clarity with regard to the reservoir and source potential. In conjunction with comparing the organic material present in the microbialites and surrounding facies, there have been few attempts to interpret the heterogeneity of extractable organic matter preserved in the microbialites and associated mudstone, dolomitic marlstone, oolitic grainstone and peloidal wackestone to packstone as a function of depositional processes. Understanding the types, abundances, and distributions of preserved organic matter in these rocks as a function of depositional processes is vital for providing a predictive framework for exploring and identifying microbialite reservoirs within similar systems.

Previous studies on the Green River Formation have been centered on understanding the depositional environment, stratigraphy, effects of climate and tectonics on sedimentation, thermal maturity, and source of organic matter. This project took a new

approach, using organic geochemistry to establish differences in reservoir and source potential between the microbialites and associated facies. Through critical assessment of the organic geochemistry, specifically the extractable organic material and Total Organic Carbon (TOC) present in the samples, the microbialites can be distinguished from the surrounding lacustrine carbonates. TOC, along with type and source of organic matter, is important in assessing the petroleum generative potential and reservoir potential of a rock. Analyzing the data from these parameters provides geochemical insight into the microbial carbonates potential to act as a petroleum reservoir and source rocks.

1.2 Geologic Background

The Eocene Green River Formation (GRF) was deposited in two large paleo-lake complexes known as Lake Uinta and Lake Gosiute (Donnell, 1965) (Figure 1.1). This continental lake system covered most of present-day western Colorado, northeastern Utah, and southwestern Wyoming. Lake Gosiute occupied the greater Green River Basin in Wyoming, whereas Lake Uinta covered much of northern Utah and western Colorado (Figure 1.1). The Gros Ventre, Wind River, and Sweetwater uplifts bordered Lake Gosiute and Lake Uinta on the east (Donnell, 1965). The Uinta Uplift, an east-west-trending high, was positive during most of the early to middle Eocene, contributing sediments to Lake Gosiute and Lake Uinta, and forming an effective barrier between them (Donnell, 1965). Both of these paleolakes were terminal, with no outlets. They were characterized by fluctuating lake levels for most of their depositional history (Bradley, 1964). Although not rift basins as is Santos basin, the Green River, Uinta and Piceance basins all resemble the "sag" phase of the pre-salt in that they are very broad, rapidly subsiding basins (Awramik

and Buchheim, 2012) making the Green River formation a suitable analog to understand the controls on reservoir and source potential for lacustrine microbialites.

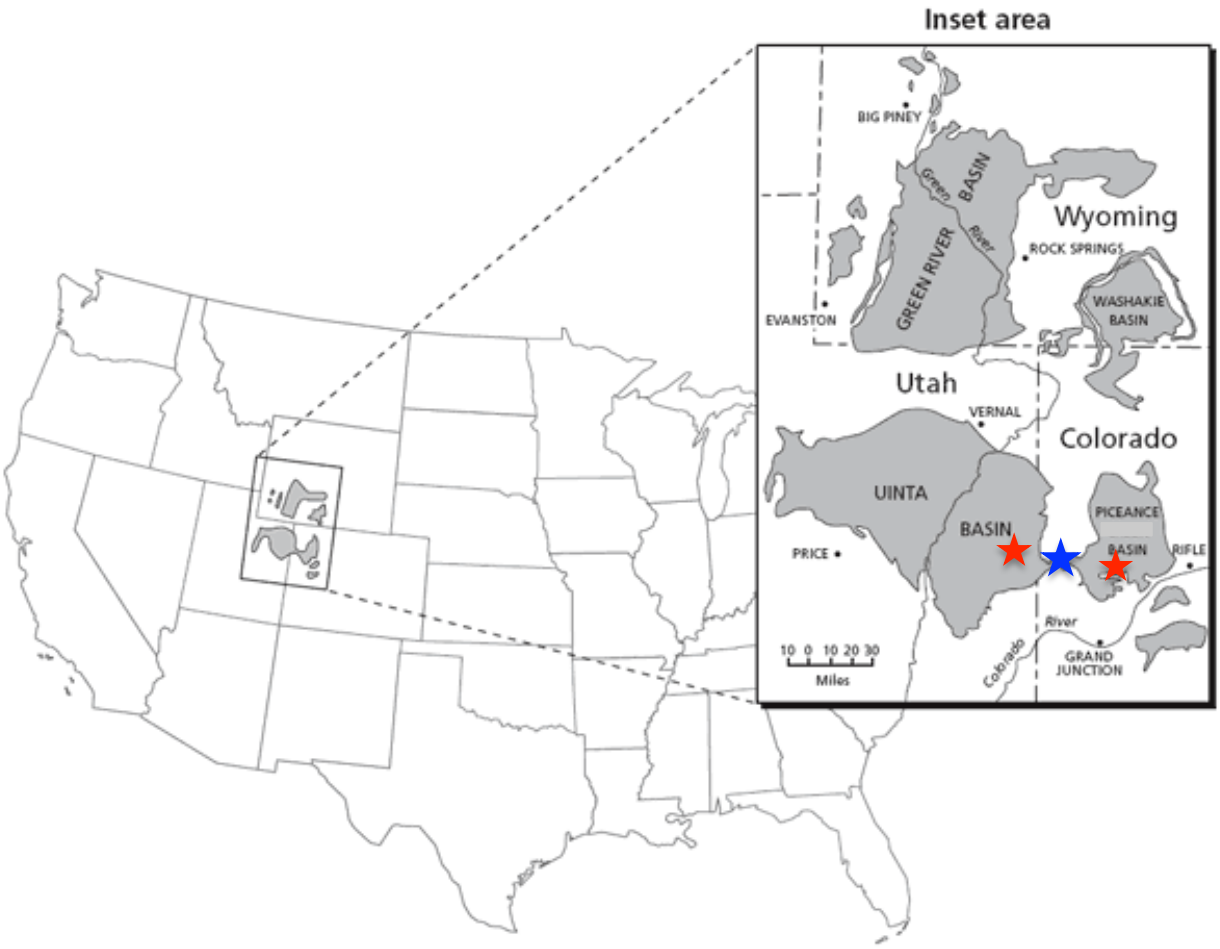

Figure 1.1: Map of the basins of the Green River Formation with core localities studied denoted by the red stars. The Douglas Creek Arch outcrop sampling location is denoted by the blue star. The core from Uinta Basin is in the more marginal area of the basin where the core from Piceance Basin is closer to the depocenter. Modified from Smith, 1980.

There have been two end-member depositional models proposed aiming to describe the evolution and formation of organic rich deposits in the Green River Formation: the stratified lake model and the playa lake model. The stratified lake model, proposed by Bradley and Eugster (1969), suggests the lake was permanently stratified, divided into a

lower, highly reducing, sodium-and bi-carbonate rich saline zone overlain by a less saline oxidizing zone. This model also suggests that algal blooms would utilize most of the CO_2 in the water causing the pH to increase resulting in the precipitation of minute calcite crystals. Upon death, the planktonic algae along with the calcite crystals settled through the lower saline layer and onto the lake bottom to produce alternating organic-rich and carbonate-rich laminae due to the difference in specific weights of the algae and calcite grains. This model suggests calcite crystals would be the dominant carbonate phase. However, the major criticism with this model is that dolomite (rather than calcite) is the dominant carbonate phase identified in the oil shales of the Green River Formation.

To explain the dilemma of dolomite rather than calcite being the dominant carbonate phase in oil shale, Eugster and Surdam (1973) proposed a playa-lake model. In this model, broad playa-like flats surrounded a relatively shallow saline lake (Johnson, 1981). In the playa-lake model, calcite precipitates due to the evaporation of ground water in the playa flats, thus causing the Mg:Ca ratio to increase until dolomite begins to precipitate. During wetter periods, algal blooms occurred due to lower salinity contents in the water. Then, as the salinity of the lake increased, metazoan grazers died out due to the harsh oxygen lean conditions of the water, causing the microbial mats generated during the algal blooms to be preserved in the rock record (Riding, 2000; 2010; 20011). Microbial mats act as the accreting surface for most stromatolites and other benthic microbialites (thrombolites, dendrolites, and leiolites), which are the mineralized structures of these microbial mats (Riding, 2000). Previous interpretations that paleo-lake Uinta was hypersaline with anoxic bottom waters limiting the competition from metazoan grazers explain the abundance of microbialites, stromatolites, and thrombolites in the Green River

Formation (Buchheim et al., 2012; Sarg et al., 2013). More evidence consistent with the playa-lake model was provided by Surdam (1975), who discovered Magadi-type chert ($NaSi_7O_{13}(OH)_3$ x 3 H_2O), a hydrous sodium silicate interpreted to represent seasonal stratification (Behr, 2000). Magadi-type chert, along with the observations of desiccation features and mudcracks, indicated that there was a closed, stratified lake surrounded by playa flats subject to periods of subaerial exposure (Surdam, 1975).

1.2.1 Study Area and Stratigraphy

This study focused on examining strata from two basins: the Uinta and Piceance Creek basins (Figure 1.1). The Douglas Creek Arch, a north-trending anticline that connects the Uinta Mountains and the Uncompahgre Plateau, acted as a physical barrier splitting Lake Uinta into the Uinta Basin in Utah and the Piceance Basin in Colorado (Johnson, 1985). Samples were selected from the Parachute Creek Member and the Garden Gulch Member (both parts of the Green River Formation) from the Piceance Basin core (Figure 1.2). The Parachute Creek Member consists mainly of finely laminated dolomitic "oil shale" interbedded with sparse siltstone and sandstone beds, and bedded and disseminated evaporites (Tänavsuu-Milkeviciene and Sarg, 2012). Surprisingly, very seldom are the "oil shales" of the Green River Formation actually shales (Dean, 1973). Instead, the most dominant lithology of the "oil shales" is dolomitic marlstone, which belies the complexity of the rock with a simplified nomenclature (Dean and Anders, 1991). The dolomitic marlstones of the Green River Formation are a mixture of almost every combination of carbonate minerals in the system Ca-Mg-Fe-CO_3 (Desborough and Pitman, 1974; Desborough, 1978). The upper part of the Parachute Creek Member interfingers with the

alluvial, deltaic and turbidite deposits of the Uinta Formation (Tänavsuu-Milkeviciene and Sarg, 2012). The dominant carbonate lithology of the rocks of the Parachute Creek Member at Douglas Pass is in the form of laterally linked hemispheroids of algal origin (stromatolites) (Cole and Picard, 1978). The stromatolite beds range in thickness from 1 cm to 5 cm and commonly are interstratified with calcareous claystone or siltstone (marlstone) (Cole and Picard, 1978). The Garden Gulch Member is dominated by illitic (clay-rich) oil shale deposits (Tänavsuu-Milkeviciene and Sarg, 2012).

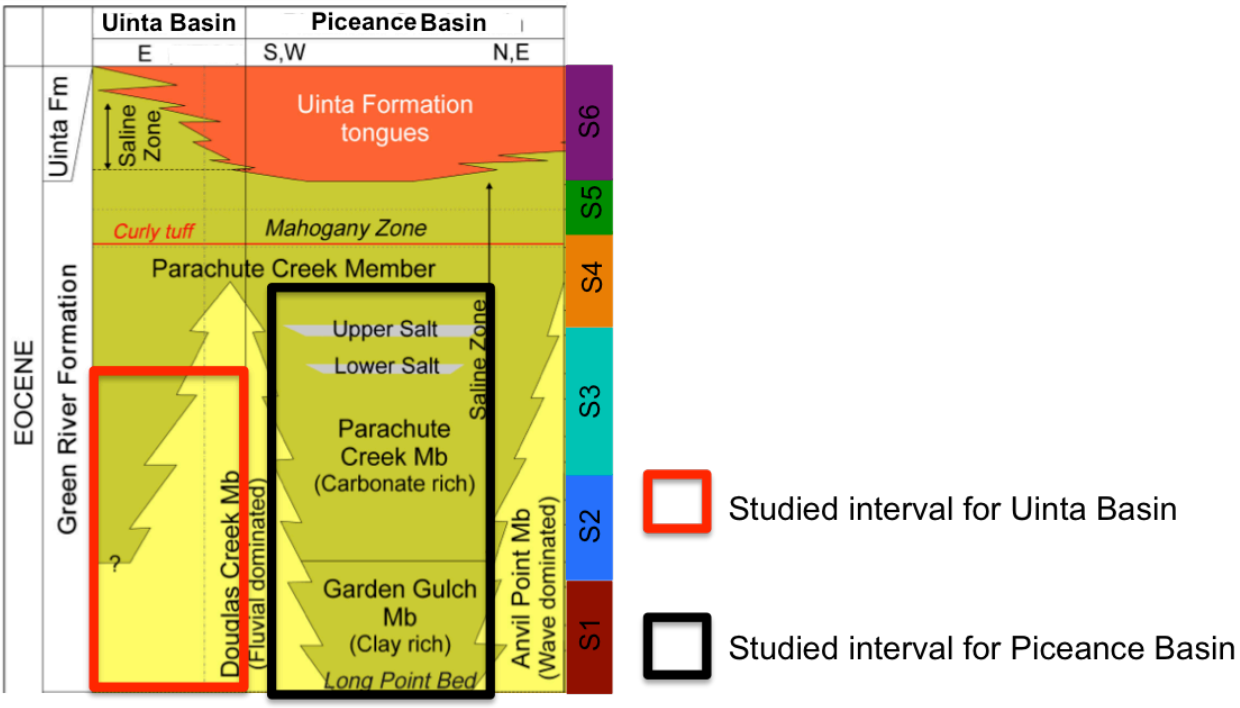

Figure 1.2**:** Generalized Green River Stratigraphy with associated lake stages for paleo lake Uinta. S1, S2, S3, S4, S5, and S6 denote the lake stages of lake Uinta. Note the samples studied in the Piceance Basin span lake stages 1 through 4 while those from Uinta span 1 through 3. Also the formations studied from each Basin differed with the Douglas Creek Member being analyzed from the Uinta Basin while the Garden Gulch, and Parachute Creek Members were analyzed. Modified from Tänavsuu-Milkeviciene and Sarg (2012) and Huang and Bartov (2012).

The Douglas Creek Member of the Uinta Basin and Douglas Creek Arch was sampled in both core and outcrop for analysis. On the Douglas Creek Arch at Douglas Pass, the rock types of the Douglas Creek Member are dominated calcitic and dolomitic mudstone, algal boundstone, oolitic grainstone, pisolitic limestone, siliciclastic mudstone, and sandstone, interpreted to represent marginal lacustrine facies (Cole, 1985; Moncure and Surdam, 1980; Sarg, 2013; Young, 1995). At Douglas Pass, these facies commonly form upward-deepening cycles that start with sharp-based grainstone and packstone, overlain by stromatolites or thrombolites, and capped by fine-grained stromatolites (Sarg, et al., 2013) (Figure 1.3).

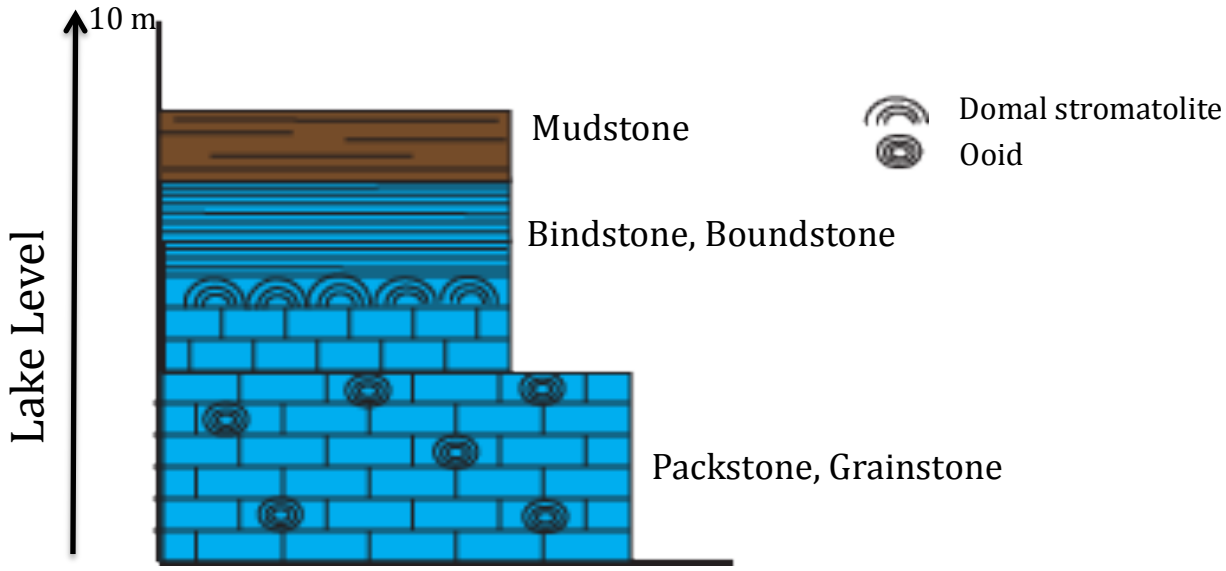

Figure 1.3: Idealized deepening-upward carbonate succession for Douglas Creek Member at Douglas Pass. Note the domal stromatolites are much thinner (<1m) in relation to the fine-grained stromatolites (3 m). Modified from Sarg et al., 2013.

Roehler (1974) points out some of the original members of the Green River Formation are actually lateral equivalents. For example, at Douglas Pass where Bradley (1931) originally described the type section of the Douglas Creek Member, Roehler (1974)

demonstrated that most of the member is actually time correlative with the lower and middle parts of the Parachute Creek Member in other parts of the basin. To overcome the nomenclature and correlation problems, Cole (1978) split the Douglas Creek Member into two informal units, the basal "sandstone facies" and the overlying "stromatolite facies." Successions similar to these have been described in the Uinta Basin (Ryder 1976; Williamson and Picard 1974).

1.3 Lake Evolution

A detailed stratigraphic study (Johnson 1985), aimed at understanding and defining the evolution of lakes in the Uinta and Piceance basins, measured sections at Evacuation Creek in the easternmost part of the Uinta Basin. The results of the study suggest a division of the Green River Formation into five depositional stages.

Lake stage 1 began with an overall rise in the lake level, marked by the deposition of the Long Point Bed at the base of the Green River Formation. During this stage, low-grade oil shales were deposited in both the Uinta and Piceance lakes near the depositional centers of each basin, and siliciclastics at the margins. Magadi-type chert occurs in sediments of this stage, which indicates that the lake could have been chemically stratified (Eugster, 1967). The upper boundary of stage 1 is characterized by the deposition of thin microbialites and Magadi type chert along the western margin of the lake in Piceance Basin (where the core sampled). Lake stage 2 is marked by an increase in oil shale richness (77.5 to 155 liters per metric ton) and multiple episodes of lake level rise and fall. During stage 2, the oil shales are illite dominated and carbonate poor, much like during the first stage. The character of sedimentation fluctuated dramatically during stage 2, between periods of

rapid clastic sedimentation during which thick clastic wedges penetrated into the profundal oil shales, depositing organically leaner zones, and periods of slow clastic sedimentation, during which stromatolites dominated. Lake stage 3 was a period of fluctuating lake levels and an increase in salinity, with a shift to more carbonate-rich deposits. The first appearance of nahcolite ($NaHCO_3$), a colorless bicarbonate mineral that forms in association with the oil shale in high salinity, occurs in stage 3 strata. This interval can be correlated into the adjacent Uinta Basin, where it is represented by a more interbedded clay-rich and carbonate-rich succession with no evidence of nahcolite deposition. The shift to more carbonate-rich deposition is most evident in the marginal areas of both the Piceance and Uinta basins, where the thick clastic intervals deposited in stage 2 are overlain with 30-60 m thick interval of stromatolites and carbonate-rich mudstone (Johnson, 1985). Lake stage 4 was marked by a minor lake level rise, just enough to deposit oil shale over the outer marginal shelf areas, including Douglas Creek Arch. As a result, in the Piceance basin, thick and continuous deposits of rich oil shale occur. In the Uinta basin, deposition of oil shales was interrupted by deposition of mudstone, siltstone and sandstone beds. The interval from this stage in the Uinta Basin is considerably thicker than in the Piceance Basin and hence the dilution by clastics may be largely responsible for the leaner oil shale deposits (Johnson, 1985). Lake stage 5 was a period in which the lake reached its maximum depth represented by the deposition of the Mahogany zone, the most extensive oil-shale rich zone (Johnson, 1985). Following this maximum flooding event, the lake began to be filled in first by lacustrine and fluvial sediments then lastly volcaniclastic sediment of the Uinta Formation (Johnson, 1985).

Although the five stage division is used commonly and widely, Tänavsuu-Milkeviciene and Sarg (2012) divide the lake evolution into six stages based on the detailed study of facies associations, depositional trends, gamma ray and Fischer assay data of the Uinta-Piceance lakes. The main difference in the five stage division done by Johnson (1985) and the six stage division by Tänavsuu-Milkeviciene and Sarg (2012) is the implementation of a sequence stratigraphic framework coupled with Fischer Assay data and Gamma Ray data as basis for defining the lake evolution. The lakes are identified by basin because paleo-lake Uinta was two independent lake systems, separated by the Douglas Creek Arch. These ancient lakes, however, acted independently, leading to unique depositional histories and lake chemistries (Pitman, 1996). The six stages defined by Tänavsuu-Milkeviciene and Sarg 2012 are referred to (with interpretations) as S1 Fresh Lake, S2 Transitional Lake, S3 Highly Fluctuating Lake, S4 Rising Lake, S5 High Lake, and S6 Closing Lake. The key difference between this framework and the existing subdivisions is that stages 5 and 6 were split into two by Tänavsuu-Milkeviciene and Sarg (2012) based on the identification of a sequence boundary. The lake stage evolution proposed by Tänavsuu-Milkeviciene and Sarg (2012) suggests that the six defined lake stages correlate with warming and cooling events identified by the early to middle Eocene global climate reconstruction of Zachos et al. (2001, 2008). According to a study (Feng et al., 2012), the six lake stages of Lake Uinta correlate with the early to middle Eocene climate optimum. Feng et al. (2012) correlate the lake stages with the respective climate at time of deposition: S1 formed during the warming phase of the climate optimum and is representative of the evolution from fresh water to saline conditions. From S1 to S2, there was a transition from an open lake to a closed lake, suggesting less abundant rainfall, with a more seasonal and dryer climate

(Tänavsuu-Milkeviciene and Sarg, 2012) (Feng et al., 2012). Feng et al. (2012) interpreted increased seasonality and flashy runoff that started during S2 were represented by restricted lake conditions. The climate was the driest during S3, the stage in which nahcolite and halite are abundant (Tänavsuu-Milkeviciene and Sarg, 2012; Feng et al., 2012). The ensuing lake level rise in S4 and the eventual maximum lake level in S5 occurred during the climactic cooling, which was accompanied by an increase in precipitation (Feng et al., 2012). Put simply, the paleotopographic high of Douglas Creek Arch, in combination with temporal variations in lake level and sediment supply as controlled by local tectonics and climate, controlled lake chemistry, evolution, and the facies preserved in each basin respectively (Carroll and Bohacs, 1999).

1.4 Microbial Carbonates

Microbialites are "organosedimentary deposits that have accreted as a result of a benthic microbial community trapping and binding detrital sediment and forming the locus of mineral precipitation" (Burne and Moore, 1987). Microbialites are "rocks" that are produced, induced or influenced by benthic microbial communities, primarily bacteria and sometimes diatoms (Dupraz, 2009). The term "microbialite" has been most widely used to describe stromatolites, thrombolites, oncolites, dendrolites, and leiolites (Dupraz, 2009). The most common variations observed in the Green river are stromatolites and thrombolites. Microbialites can be found in a broad range of environments including open marine as in some Bahamian stromatolites, supratidal, hypersaline and saline environments, freshwater and alkaline settings, and there are even some subaerial stromatolites (Riding, 2000). Their various classifications are based on their internal

structures: stromatolites have a laminated fabric, thrombolites a clotted fabric, oncolites a concentric fabric, leiolites an aphanitic fabric, and dendrolites a dendritic fabric (Riding, 2000).

Stromatolites can exhibit various morphologies ranging from simple domal structures to complex branching digitate structures (Riding, 2000, 2011, 2006; Sarg et al., 2013). They first appear in the rock record around 3.4 Ga (Awramik and Sprinkle, 1999). Whereas Archean and Proterozoic strata contain a great abundance and diversity of stromatolites, there is a dramatic decline in the early Phanerozoic due to diversification of metazoans (Awramik and Sprinkle, 1999). There has been debate on the mechanism of formation of stromatolites ever since Kalkowsky first described them in 1908. Most scientists suggest that they result from the action of microbial mats trapping, binding and precipitating minerals (Walter, 1976). Yet, numerical models demonstrate the possibility of abiotic precipitation as the mechanism for forming stromatolites (Grotzinger and Rothman, 1996). However, insomuch as microorganisms exist virtually in all shallow water environments, it would be misleading to discount them inhabiting the surfaces of most, if not all stromatolites (Grotzinger and Rothman, 1996). Although microorganisms may have inhabited the surfaces of most, if not all stromatolites it is not clear-cut as to what role they played in the formation of stromatolites (Grotzinger and Rothman, 1996). So it remains necessary to remain cautious in assuming biogenicity without direct evidence in the form of fossilized microbes that can be shown to have influenced the morphogenesis of the stromatolite (Grotzinger and Rothman, 1996).

Aside from stromatolites, thrombolites, the other morphology of microbial carbonates present in the Green River Formation, are cryptalgal structures related to

stromatolites, but lacking lamination and characterized by a macroscopic clotted fabric (Aitken, 1967). Thrombolites were prominent during the Proterozoic and throughout the much of the Cambrian and early Ordovician (e.g., Armella, 1994; Kennard, 1994; Riding, 2000). Some thrombolites as stromatolites are produced as a result of microbial calcification or agglutination (Riding, 2000). They appear to be essentially subtidal and form columns, domes, layers and thick crusts (e.g. Pratt and James, 1982; Riding et al., 1991b; Armella, 1994; Kennard, 1994), but are characteristically domical meter-scale doughnut-like masses (Luchinina, 1973; Rowland and Gangloff, 1988)(Riding, 2000). There are two main classifications of thrombolites: calcified microbial thrombolites and coarse agglutinated thrombolites. The calcified microbial thrombolite fabric can be produced by microbial calcification, typically displaying well-defined clots that probably were formed by cyanobacteria (Riding, 2000). Coarse agglutinated thrombolites incorporate sand- and even gravel-sized oolitic and bioclastic sediment, and commonly exhibit complex internal variation that includes stromatolitic, crudely layered blotchy, or relatively structureless fabrics (Riding, 2000).

Two other morphologies that are seldom found in the Green River Formation are dendrolites and leiolites. Dendrolites have a macroscopic centimetric bush-like fabric, typically produced by calcified microbes similar to thrombolites (Riding, 2000). Dendrolites acted as major reef builders on their own or in conjunction with sponges in the Cambrian to early Ordovician and stromatoporoids in the Devonian (Mountjoy and Riding, 1981)(Riding, 2000). Leiolites have a relatively structureless, aphanitic, macrofabric lacking clear lamination, clots or dendritic fabrics (Riding, 2000). The term is founded on

examples in the Late Miocene of Southeast Spain (Braga et al., 1995) where leiolites form large domes in association with stromatolites and thrombolites (Riding, 2000).

Although the biogenicity of 3.4 Ga stromatolites has been questioned (Buick et al., 1981; Lowe, 1994; Grotzinger and Knoll, 1999; Lindsay et al., 2003), all modern microbialites called stromatolites are associated with microbial communities that induce, or serve as organic substrate for, precipitation (Riding, 2000). The debates on biogenicity mainly focus on whether laminae or morphology can uniquely reflect biology (e.g., Grotzinger and Rothman, 1996; Knoll and Grotzinger, 1995). However, it is still standard to identify microbialites based on the method outlined by Riding, (2000): microbial carbonates are distinguished based on their meso-fabrics (internal fabrics), and macro-fabrics (e.g., laminated, clotted, dendrolitic, and aphanitic) that characterize the major categories and varieties of microbial carbonate. The majority of modern stromatolites occur in hypersaline and open marine environments because the microbial communities can survive the higher salinities, whereas most eukaryotes, such as macroalgae and burrowing or grazing invertebrates which compete with or ingest cyanobacteria and disrupt lamination, are largely excluded (Fischer, 1965; Awramik, 1971, 1982, 1992; Walter and Heys, 1985; Riding, 2006; Dupraz, 2009).

1.5 Biomarkers

Biomarkers are complex molecular fossils derived from biochemicals, particularly lipids, synthesized by once living organisms (Peters et al., 2005a). Various factors, such as type of organic matter input, redox potential during sedimentation, bioturbation, sediment grain size, and sedimentation rate, influence the quantity and quality of organic matter

preserved in the rock record, which in turn effects the detectability of various biomarkers (Peters et al., 2005a). Extractable organic matter, commonly referred to as bitumen, is composed of hydrocarbons that are soluble in organic solvents (Killops and Killops, 2009). This extractable organic matter can contain various compounds such as paraffins, which includes *n*-alkanes (Figure 1.4), *iso*-alkanes, *anteiso*-alkanes, napthenes (cyclo-alkanes), aromatic hydrocarbons, sulfur-containing aromatic hydrocarbons, and lipid biomarkers, which are preserved biosynthesized molecules, such as carotenoids, biopolymers, or cell membrane components (Killops and Killops, 2009). It is well known that the use of these compounds can aid in determining paleoenvironments (Peters et al., 2005b). However, beyond this use, these compounds also can aid in determining the reservoir and source potential of the lacustrine microbialites. Industry-standard metrics for describing compounds include the terrigenous/aquatic ratio (TAR), odd over even predominance (OEP) (*n*-alkanes), the sterane/hopane ratio, % (C_{27}, C_{28}, C_{29}) Sterane, and the Pristane(Pr)/Phytane(Ph) ratio.

Different organisms synthesize different types of molecules, thus the biomarkers preserved in a rock can be used to infer what organisms were present at deposition. As molecules break down uniquely during diagenesis, molecular structure observed in the preserved biomarker can be used to determine the maximum diagenetic temperature/pressure (thermal maturity) experienced during burial in a rock or oil. There are a variety of biomarkers (hopanes, steranes, and terpanes) that can aid in determining the source and maturity of the organic matter. In particular, polycyclic structures, hopanes and steranes are used widely as sedimentary fingerprints for bacterial and eukaryotic source inputs (Talbot et al., 2003; Volkman, 2005) (Siljeström, 2010).

Hopanes (Figure 1.4) originate almost exclusively from hopanepolyols present in the cell membranes of many prokaryotes (bacteria), whereas steranes mainly originate from sterols that modify the cell membranes of Eukaryota (consisting mainly of algae and higher plants) (Rohmer et al., 1984; Peters et al., 2005; Volkman, 2005)(Siljeström, 2010). Hopanes range in chain length from C_{27} to C_{35} molecules and are divided into normal hopanes (C_{27}-C_{30}) and homohopanes (C_{31}-C_{35}) (Peters et al., 2005b). Gammacerane, a C_{30} triterpane, is used frequently as an indicator of water column stratification (e.g., Sinninghe Damsté et al., 1995).

Within source rocks and crude oils, derivatives of eukaryote-cell-wall steroids called steranes identified by their characteristic ion-mass to ion-charge (m/z) number (m/z 217) are represented by C_{27}, C_{28}, and C_{29} molecules (Figure 1.4). Yet, each has different origins. C_{27} steranes originate predominantly from marine algae; C_{28} steranes from yeast, fungi, bacterial plankton, and algae; and C_{29} steranes from land plants (Peters et al., 2005b). The sterane composition and biological source of ancient sediments are related (Huang and Meinschein 1979; Volkman 2003) and can be assessed by examining the percentage of each sterane to indicate the primary source of organic matter. The sterane/hopane ratio reflects the relative input of eukaryotic (consisting of mainly algae and higher plants) versus prokaryotic (bacteria) organisms to the source rock (Peters et al., 2005b).

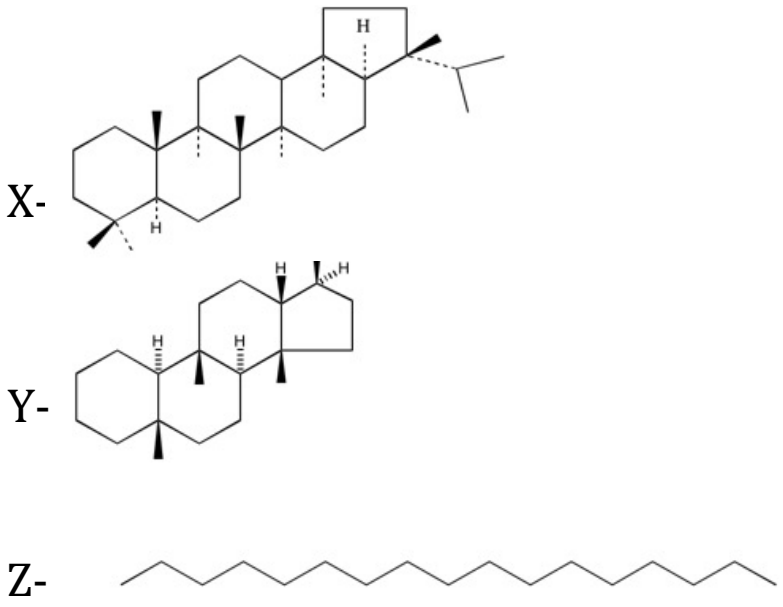

Figure 1.4: Structures of major compounds used for source and reservoir analysis. X= Hopane, Y= Sterane, and Z= *n*-alkane (after Grantham, 1985 and Prince, 1994). X is a generalized molecular structure of a Hopane composed of four cyclohexane rings and one cyclopentane ring. Y is a generalized molecular structure of a Sterane made up of an androstane skeleton composed of Carbon and Hydrogen. Z is a generalized structure of an *n*-alkane (*n*-C_{17}), which is composed of Carbon atoms.

Once the extractable organic matter is extracted from each sample using organic solvents, the resulting mixture can be analyzed with a gas chromatogram/mass spectrometer (GC/MS). As biomarkers fragment in known and characteristic ways (Gallegos, 1973), their chemical structures can be identified using the retention time in the GC as well as their unique fragmentation pattern in the MS. Different suites of biomarkers can also be identified using their characteristic ion-mass to ion-charge (m/z) number. For instance, hopanes (m/z 191), steranes (m/z 217), *n*-alkanes (m/z 85), and aromatics (m/z 131) can all be identified this way.

1.6 Source Potential

Accurate assessment of the source potential of strata requires describing a number of variables, including type, source, quantity, and thermal maturity of the associated organic matter. However, one of the most important variables is the wt % TOC contained in the rock. If TOC is >2% within a rock it is classified as a prolific source rock (Peters and Cassa, 1994). However, within strata classified by the general term "source rock" exists different variations source quality based on the attributes of the organic matter in the rock. These variations include source rocks, effective source rocks, potential source rocks, active source rocks, inactive source rocks, and spent oil source rocks (Peters and Cassa, 1994). Thus, there are various methods or geochemical screening techniques by which to evaluate the petroleum generative potential of a rock unit. The most commonly used and effective methods are Rock-Eval pyrolysis and TOC measurements, which can be supplemented with vitrinite reflectance data and spore coloration data for a more precise assessment of the petroleum generative potential of a specific rock unit (Peters and Cassa, 1994). The Rock-Eval pyrolysis method consists of a programmed heating of a small sample within an inert atmosphere to selectively determine the free hydrocarbons, or the hydrocarbon- and oxygen-bearing compounds that are volatilized during the cracking of the unextractable organic matter or kerogen (Peters and Cassa, 1994). TOC describes the quantity of organic carbon in a rock sample and includes both kerogen and bitumen (Peters and Cassa, 1994). There are various methods for determining TOC that are more efficient depending on sample size. Although TOC is an effective method for indicating organic richness of source rocks, it is not always an exact or clear indicator, in that some rocks may contain a large amount of carbon, but are unable to generate petroleum. For example, a deltaic marine

shale may contain up to 5 wt. % TOC, but contain gas prone or inert organic matter, making it a very unlikely candidate to yield petroleum. Thus, high TOC alone is not a definitive measure of source potential, but combining this measure with data on the type and source of extracted organic matter provides insight into the potential for hydrocarbon generation.

CHAPTER TWO: Sample Collection and Methods

2.1 Field Sampling Site

The Douglas Creek Arch, which connects the Uinta Mountains and the Uncompahgre Plateau, separates paleo-Lake Uinta into the Uinta Basin in Utah and the Piceance Basin in Colorado (Figure 1.1) (Moncure and Surdam, 1980; Cole, 1985; Young, 1995). On the Douglas Creek Arch, the rock types of the GRF are dominated by facies characterized by calcitic and dolomitic mudstone, algal boundstone, oolitic grainstone, pisolitic limestone, siliciclastic mudstone, and sandstone (Figures 2.1 and 2.2) (Cole, 1985; Moncure and Surdam, 1980; Young, 1995). These facies are interpreted to represent marginal lacustrine deposits (Cole, 1978).

Figure 2.1**:** Field photo of a domal stromatolite that was sampled from the Douglas Creek Member at Douglas Pass. The head of the hammer for scale is 18 cm in length and 2.5 cm in height. Notice that although the stromatolite is domal it has a very finely laminated macro-texture.

Figure 2.2**:** Polished slab from core drilled through the Douglas Creek Member showing a fine-grained stromatolite with very low relief laterally linked hemispheroids. Figure is taken directly from Figure 10 of Sarg et al. (2013). Fine-grained stromatolites are the main type of microbialite identified in core for both the Uinta and Piceance basins.

2.2 Sample Collection

A total of 19 samples were collected from cores in the Piceance and Uinta basins (Figure 1.1). At all localities, both microbial carbonate and associated lacustrine lithofacies were sampled (Table 2.1).

Sample #	Sample Lithology
B987 3111	Fine-grained stromatolite
B987 3201.8	Mudstone
B987 3202.7	Mudstone
B987 3231.8	Marlstone
B987 3397.4	Fine-grained stromatolite
B987 3432.7	Fine-grained stromatolite
B987 3437.9	Thrombolite
Douglas Pass	Domal Stromatolite
Douglas Pass	Marlstone
Douglas Pass	Ooid grainstone
B824 1363	Fine-grained stromatolite
B824 1367	Dolomitic oil shale
E055 1362.7	Siltstone
E055 1383.4	Dolomitic oil shale
E055 1540.2	Oil shale breccia
E055 1549.6	Dolomitic oil shale
E055 1751.4	Evaporite with nahcolite
E055 1769.4	Fine-grained stromatolite
E055 1774.8	Fine-grained stromatolite
E055 2525.2	Fine-grained stromatolite
E055 2535.5	Fine-grained stromatolite
E055 2709.8	Thrombolite

Table 2.1: Samples collected from core and outcrop for analysis. Cores include equal sampling of microbial carbonates and associated lacustrine carbonates (mudstone, marlstone, dolomitic oil shale, oil shale breccia, and ooid grainstone). The B987 samples are from a core that was taken in Uinta Basin, while the E055 and B824 samples were taken from cores representing Piceance Basin sediments.

2.3 Sample Preparation

Core samples, each around 2.54 cm x 2.54 cm dried at room temperature. Each sample was then placed in a mechanical ball mill grinder for a duration of ~10 minutes at 225 rpm to collect ~5 g of sample for analysis. After each sample was crushed and put into a combusted glass container, the ball mill and all components are solvent washed with hexane to remove any contamination between samples.

2.3.1 Organic Material Extraction

Prior to extraction, all glassware was combusted overnight at 450 °C to remove any contaminants. Once powdered, each sample was extracted using a 9:1 (v:v) mixture of dichloromethane (DCM): methanol (MeOH) in a microwave-accelerated reaction system (MARS, 100°C, 800 W, 40 min extraction) to remove all of the extractable organic material from the sample. After extraction, each sample was vacuum filtered to obtain only the liquid extract for analysis. These extracts were then reacted with activated copper to remove any traces of elemental sulfur present in the samples. This process consists of taking a glass pipette and placing combusted glass wool in the bottom to create a filtration effect. Then, activated copper powder was added to the column. The extracted sample of about 2-5 mL was pipetted onto the top of the copper and allowed to permeate through the copper before allowing 4-5 column volumes of DCM to run through the column. After reaction with the activated copper, each sample was evaporated down to about 1 mL for placement in a GC vial. After one GC run, silica gel chromatography was performed. This process also consists of taking a glass pipette and placing combusted glass wool at the bottom to create a filtration effect for the sample. Then, silica gel was added to the column and packed with gentle tapping to eliminate any voids in the silica gel that might serve as preferential flow paths. Before pipetting the sample into the silica gel column the dead volume had to be determined by pipetting 0.5 mL of hexane at a time until the first drop reached the tip of the column. Then, the concentrated extract that was recovered after the elemental sulfur extraction was pipetted onto the top of the silica gel column and allowed to permeate into the silica gel before eluting the polar, aromatic and saturate fractions by 3 sequential additions of known solvent amounts. The first run is 3/8 of the dead volume of

hexane to retrieve the saturate fraction, then a mixture of 2.5 dead volumes of 4:1 hexane:DCM to elute the aromatic fraction, followed by the last run of several dead volumes of 7:3 DCM:MeOH to elute the polar fraction. Once each fraction was collected in an individual 40 mL combusted VOA vial, each was blown dry in the turbo vap and then brought back up with 1 mL hexane. Each fraction was then transferred to GC vials for analysis. This lipid fractionation procedure isolated the three organic fractions, saturate, polar, and aromatic, in chromatography-grade hexane for subsequent GC/MS analysis.

2.3.2 GC/MS Methods and Analysis

Each individual fraction was analyzed on a ThermoFinnigan Trace GC-DSQ quadrapole mass spectrometer, using both full scan mode and selective-ion monitoring (SIM) mode for ions of interest. The GC oven temperature was started at 40 °C and began with a 20 °C per minute temperature ramp up to 130 °C before switching to a 5 °C temperature ramp up to the max 350 °C. Specific compounds were identified based on their specific ion-mass to ion-charge (m/z) number, relative retention time, mass spectral data, and comparison with literature data.

The individual compounds were identified based on specific chromatographic retention times. The chromatographic retention time is an indicator of compound identity because retention time increases in predictable manner with increasing chain lengths. Additionally, to ensure the correct molecular identification of each compound, I also used the mass of the molecular fragments generated by electron impact ionization in the mass spectrometer. Hopanes, steranes and *n*-alkanes all have characteristic fragmentation patterns, which was cross checked against an MS database created by the National Institute

of Standards and Technology (NIST), and which is included in the XCalibur® software of published fragmentograms.

2.4 TOC analysis

The quantity of organic matter as measured by the TOC is a commonly used quantitative parameter for determining the petroleum generation potential of a stratigraphic unit. It is used to assess the quality of source rocks and even recently has been widely used for evaluating unconventional reservoirs, by measuring the organic carbon preserved in a sample. This project uses the "Rock-Eval II plus TOC" method performed by Weatherford labs. Samples were powdered then placed in 50 mL centrifuge vials that had been weighed prior to addition of the powdered sample. About 2-5 grams of powder were added to the vial and weighed again. The samples were then put in the oven to dry for about 2 to 3 days. Once dried, the vials were weighed again. Then the decarbonation process began with the addition of 30-35 mL of 6M HCl to digest and remove carbonate from the sample. Each vial was centrifuged for 5 minutes then the supernatant liquid was poured off. This process was repeated until there was no reaction with the sample when HCl was added. Once decarbonation was complete, deionized water was used to neutralize the sample for analysis. The neutralized samples were placed in the oven to dry for 4 to 5 days. Each sample was then placed in silver capsules and weighed in µg, then combusted at 1060 °C using a Costech elemental analyzer connected via a CONFLO III to the inlet of the the ThermoFinnigan MAT 253 isotope ratio Mass Spectrometer. Output data was recorded in respect to $\delta^{13}C$ V-PDB. Instrument precision was maintained each analysis run using lab standards; USGS-24, Dorm-2, and ANU-Sucrose.

CHAPTER THREE: Results

3.1 Outcrop and Core descriptions

Two cores were sampled and described from Piceance Basin, the Nielsen 17-1 (39.968728 °N, -108.304686 °W, referred to in the text by the USGS library number (B824) drilled by Kaiser Aluminum and Colorado Core 01A (40.054067 °N, -108.334852 °W, referred to in the text by the USGS library number E055) drilled by the US Bureau of Mines. For core B824, two samples were collected for TOC and GC/MS analysis from a 4 ft. (1.22 m) interval within the Parachute Creek Member of the Green River Formation (Figure 3.1). The described interval of core spanned 20 ft. (6.10 m). The interval begins with a 6 ft. (1.83 m) succession of millimeter laminated, light to dark brown oil shale containing silt lenses. Overlying the oil shale is a 3 ft. (0.91 m) thick thinly laminated limestone interbedded with boundstone displaying flat planar to undulating laminae with low-relief laterally linked hemispheroids. The next 4 ft. (1.22 m) consist of millimeter laminated, silty, light to dark brown to grey oil shale. The oil shale passes upward into a thin 1 ft. (0.30 m) fine-grained quartz sandstone with low-angle cross-stratification and some minor hummocky cross-bedding. This unit is followed by another 3 ft. (0.91 m) horizontally laminated boundstone with flat planar to undulating laminae with very low relief hemispheroids. A 3 ft. (0.91 m) bed of millimeter laminated dark grey silty oil shale caps the interval. The boundstone containing flat planar to undulating laminae with laterally linked hemispheroids is interpreted to be a fine-grained stromatolite, which has been interpreted to suggest deeper water (Logan et al., 1964; Kruger, 1969; Cohen et al., 1997; Sarg, 2013).

Ten samples were collected from core E055 for TOC and GC/MS analysis to identify the controls of depositional environment on the reservoir and source potential (Figure 3.2). The interval of core sampled spans from a depth of 2709.8 ft. (825.95 m) to 1362.7 ft. (415.35 m), which is within the Garden Gulch and Parachute Creek members of the Green River Formation. The succession begins with a 40 ft. (12.19 m) fine to medium sandstone containing cross-stratification and soft sediment deformation features including slump and load structures. The sandstone is interbedded with a very fine sand with lenticular bedding. Overlying the interbedded sandstone and siliciclastic interval is a thinly laminated limestone bed (2.44 m thick) that is interbedded with oolitic grainstone and boundstone with domal features and massive limestones with a clotted fabric. Overlying the limestone bed is a thick (13.72 m) siliciclastic sand containing lenticular bedding and some dewatering structures. The succession of fine-grained sandstone with cross-stratification and soft sediment deformation structures, fine grained, lenticular bedded siliciclastics overlain by grainstones with vertically oriented shrub like features repeats again as a 75 ft. (22.86 m)-thick interval. Above this interval is a 15 ft. (4.57 m) thick grey massive structureless mudstone. The next 550 ft. (167.64 m) include successions of fine to medium-grained sandstone with ripples and cross-stratification that pass upward into boundstones with domal features exhibiting both laminated and clotted fabrics that are capped by fine-grained lenticular bedded siliciclastics or structureless mudstones. Over the next 100 ft. (30.48 m), beds of nahcolite occur within similar successions of fine-grained cross-stratified sandstone, grainstones and boundstones with domal features consisting of shrub like features, laminated and clotted fabrics capped by finely bedded lenticular siliciclastics, and structureless mudstones. The next interval (1650 ft. - 1300 ft. depth) (502.92 m -

396.24 m) is characterized oil shale intervals containing sub-angular to sub-rounded carbonate clasts with some nahcolite and coarse-grained structureless sandstones with load and flame structures that grade upward into parallel laminated fine to very-fine grained sandstone. The carbonates in this interval have less domal morphologies and exhibit flat planar to undulating laminae with very low relief hemispheroids.

Seven samples were collected from a core from the Uinta basin, the Coyote Wash 1 (40.02284 °N, -109.31069 °W) (USGS library number B987) drilled by USGS for TOC and GC/MS analysis (Figure 3.3). The lowest 10 ft. (3.05 m) is an interval of fine-grained sandstone with ripples, load structures and low angle cross-stratification. Overlying the sandstone is a 3 ft. (0.91 m) boundstone with a clotted fabric. Next is a 20 ft. (6.1 m) massive grey marlstone. The next 20 ft. (6.1 m) of core was too heavily sampled or missing so no facies were identified in my core logging. Following the missing section is a 2 ft. (0.61 m) section of carbonate bindstone with flat planar to undulating laminae. Overlying the bindstone is another 20 ft. (6.1 m) interval of grey massive marlstone capped by a structureless mudstone (3 ft., 0.9 m). A 30 ft. (9.14 m) fine-grained cross-stratified sandstone with ripple marks is coupled with a 40 ft. (12.19 m) interval of mud-rich medium-grained thinly bedded siliciclastics. Another 40 ft. (12.19 m) section of beige to grey massive marlstone is capped by a marly, brown fissile oil shale interval (10 ft., 3.02 m). The final trend described spans 75 ft. (22.86 m) of core. It begins with 30 ft. (9.14 m) of ooid grainstone followed by 5 ft. (1.52 m) of peloidal packstone that transitions into a boundstone with domal features, and vertically oriented shrub like features. Following the boundstone is a 15 ft. (4.57 m) succession of bindstone with flat planar to undulating laminae capped by a dark brown structureless mudstone.

The succession analyzed at Douglas Pass outcrop (Figure 3.4) started with a 10 ft. (3.05 m) interval of oolitic and peloidal packstones and grainstones followed by a boundstone with well-developed columnar and domal features with laminated and clotted fabrics (5 ft., 1.5 m). The succession graded upward into grey structureless pyritic marlstone (7 ft., 2.13 m) capped with a laminated mudstone (3 ft., 0.91 m). The boundstones with laminated and clotted fabrics displaying well-developed columns and domes are interpreted to be stromatolites and thrombolites (Rainey and Jones, 2009; Gierlowski-Kordesch, 2010) (Tänavsuu-Milkeviciene and Sarg, 2012). The occurrence of peloidal wackestones and packstones along with stromatolitic and thrombolitic boundstones suggest that the Douglas Pass was a marginal lacustrine environment with a minor rise in lake level resulting in the deposition of the fine grained marlstone and mudstone (Sarg, 2013).

The successions analyzed in cores B824 and E055 represent more distal sediments that were deposited closer to the depocenter of Piceance Basin, whereas core B987 and Douglas Pass outcrop represent marginal lacustrine deposits. The ideal deepening cycle (Figure 1.3) correlates to the marginal lacustrine deposits of core B987 and Douglas Pass in that it represents the evolutionary lake stages (Sarg, 2013). The grainstones at the beginning of the succession correlate to the initial freshwater lake, followed by thrombolites capped by laminated stromatolites correlating with a higher salinity transitional lake, capped by laminated stromatolites and mudstone represent the rising lake (Sarg, 2013).

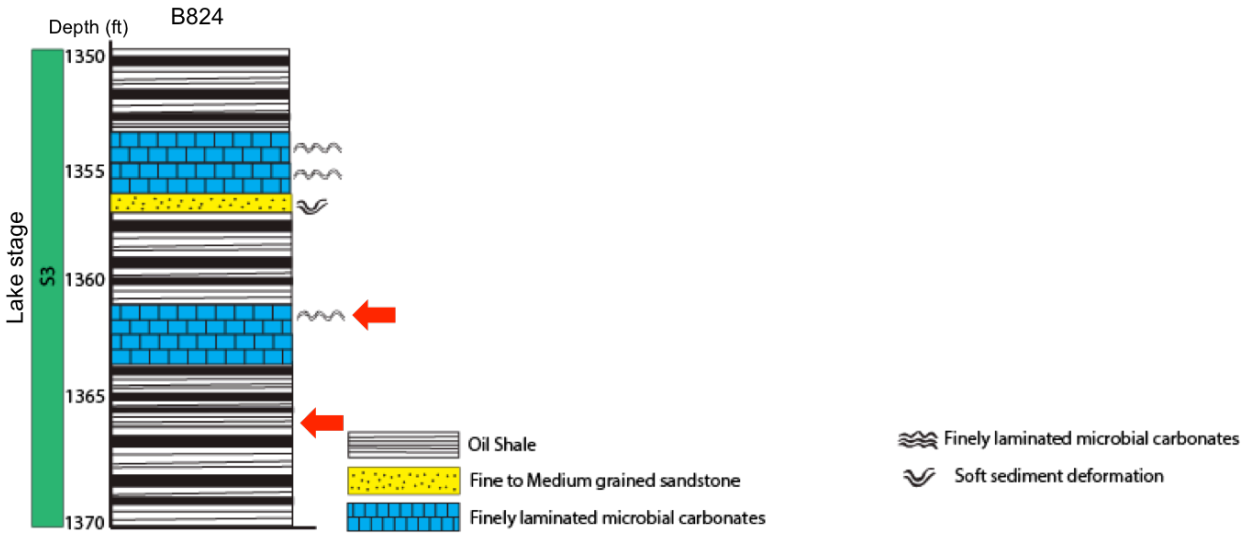

Figure 3.1: Stratigraphic column constructed from core descriptions of core B824. Notice the limited siliciclastics and abundant microbial carbonates and oil shales. “S3” refers to lake stage 3, during which the sample strata were deposited. Red arrows denote sampling location.

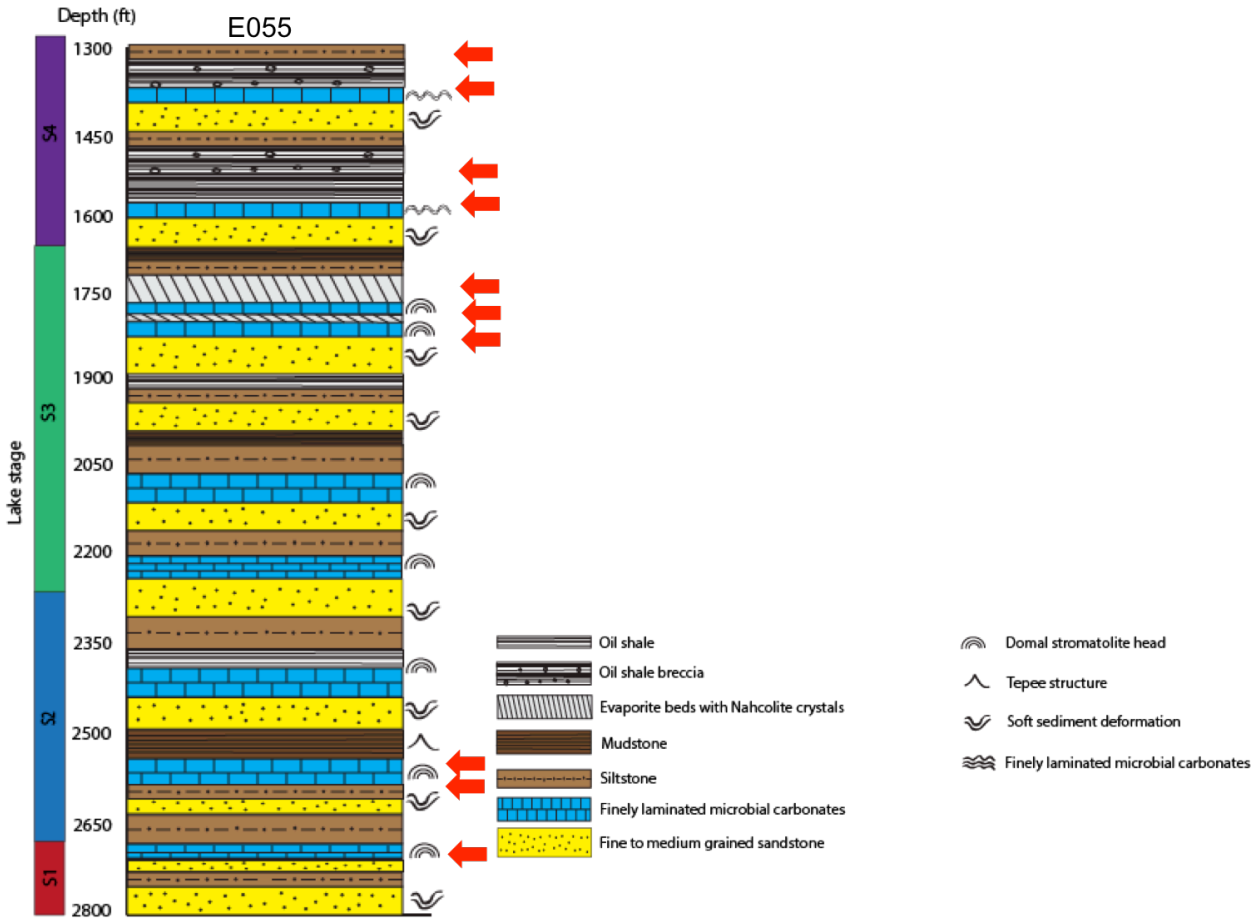

Figure 3.2: Stratigraphic column constructed from core descriptions of core E055. Notice the decrease in siliciclastic input towards the upper portion of the core. "S1, S2, S3, and S4" refer to the lake stages during which the sample strata were deposited. Red arrows denote sampling location.

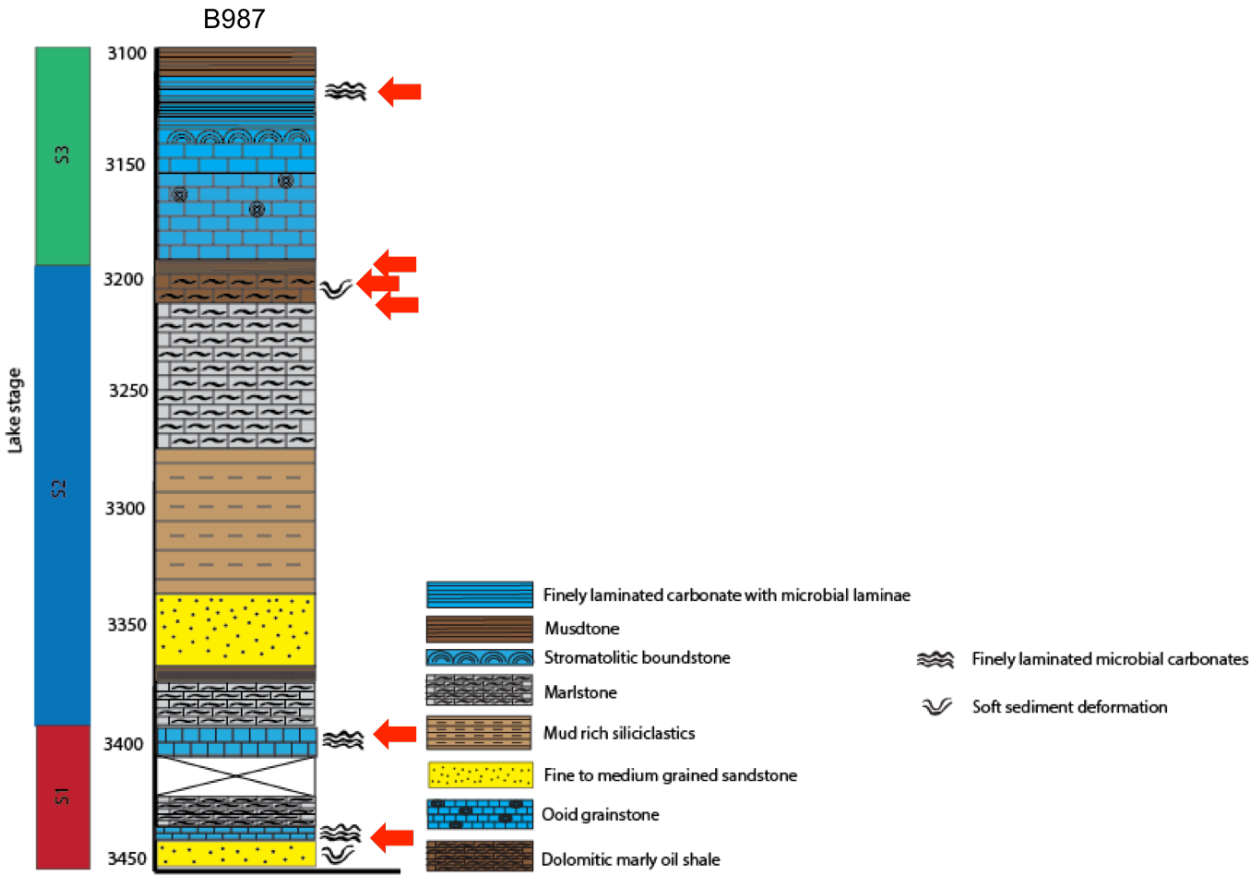

Figure 3.3: Stratigraphic column constructed from core descriptions of core B987. "S1, S2, and S3" refer to the lake stages during which with the strata were deposited. Notice the abundant siliciclastic input throughout the entire interval of the core. Red arrows denote sampling location.

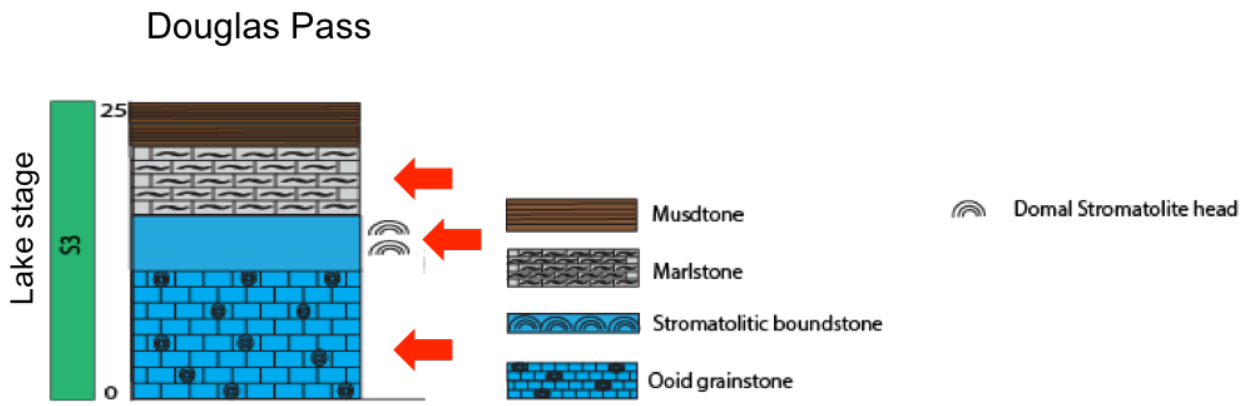

Figure 3.4: Measured section from Douglas Pass outcrop. "S3" refers to lake stage 3, the lake stage during which these strata were deposited. Note the thick succession of oolitic grainstone capped by domal stromatolites that grade into organic rich mudstones. Red arrows denote sampling location.

3.2 TOC Analysis

TOC is a bulk geochemical measurement that assesses the hydrocarbon potential of a rock based on the total organic carbon preserved. TOC values for the Uinta, Piceance and Douglas Pass samples identify various rich and lean zones. TOC values for the B987 core (Table 3.1, in the Uinta Basin) yield very low values ranging from 0.14% for core B987 at 3437.9 ft (thrombolite) deposited during lake stage 1 to 1.7% for core B987 3111 (fine-grained stromatolite), which was deposited during lake stage 3. For the outcrop samples from Douglas Pass (Table 3.1), all three samples yield low TOC values. The associated lithofacies deposited during lake stage 3 exhibited very low TOC values, 0.24% for the marlstone and 0.33% for the ooid grainstone. Although very lean, the stromatolite deposited during lake stage 3 yielded a TOC value of 0.49%. For the cores in the Piceance Basin, TOC values are much higher than those of the Uinta Basin, for both microbialites (stromatolites and thrombolites) and associated lacustrine carbonates (marlstone, ooid

grainstone, oil shale, and mudstone). For core E055 (Table 3.1), the TOC values varied among samples. For the microbialites (stromatolite and thrombolite) the values ranged from 4.52% to 28.27%, the lowest being in rocks deposited during lake stage 1, and the highest were rocks deposited in lake stage 4, with no consistent trend of increasing. The associated lithofacies, including a mudstone, oil shale and marlstone, yielded TOC values ranging from 5.38% for lake stage 3 rocks deposited in a evaporite-rich interval to 28.89% for lake stage 4 rocks. The other core (B824, Table 3.1) exhibits rich TOC values for both samples, which were deposited during lake stage 3. The fine-grained stromatolite is substantially more organic rich than the dolomitic oil shale sample with a TOC value at 39.71% compared to 29.27%. Overall, core B987 displays very low TOC values throughout the core for all lake stages, whereas cores B824 and E055 exhibit TOC values all >4%. The highest TOC values are in lake stage 3 and 4 in the cores from Piceance Basin. With TOC being key in defining source rocks these values will help to define potential of the Green River sediments.

Sample	TOC	Lake Stage
B987 3111	1.7	S3
B987 3201.8	0.28	S2
B987 3202.7	0.28	S2
B987 3231.8	0.42	S2
B987 3397.4	0.24	S2
B987 3432.7	0.48	S1
B987 3437.9	0.14	S1
Douglas Pass Marlstone	0.24	S3
Douglas Pass Ooid Grainstone	0.33	S3
Douglas Pass Stromatolite	0.49	S3
B824 1363	39.71	S3
B824 1367	29.27	S3
E055 1362.7	26.78	S4
E055 1383.4	24.93	S4
E055 1540.2	n/a	S4
E055 1549.6	28.89	S4
E055 1751.4	5.38	S3
E055 1769.4	28.87	S3
E055 1774.8	4.52	S3
E055 2525.2	26.3	S2
E055 2535.5	n/a	S2
E055 2709.8	28.27	S1

Table 3.1: TOC measurements for the Piceance and Uinta basins samples. Note the low TOC values for core B987 and Douglas Pass (<1%) in comparison with cores B824 and E055 (>5%) Samples are matched with their respective lake stage.

3.3 Biomarkers

3.3.1 N-alkanes and Isoprenoids

Within the mass-to-charge ratio (m/z = 85) n-alkanes, and the isoprenoids pristane and phytane can be identified. For *n*-alkanes the distributions within a sample can aid in

determining the origin of the organic matter. *n*-alkanes are characterized by a homologous series of short chain *n*-alkanes (e.g., nC_{15}-nC_{19}), if derived from algae, or long-chain *n*-alkanes (nC_{25}-nC_{35}), coupled with a strong predominance of odd-over-even carbon numbers, if derived from higher plant epicuticular waxes (Wakeham et al., 1980). The odd-over-even predominance (OEP) is calculated by dividing the total peak area of the nC_{21}-nC_{27} odd *n*-alkanes by the total peak area of the nC_{22}-nC_{28} even *n*-alkanes. Any value >1 is indicative of higher plant input. For core B987 (Uinta Basin), three of the four microbial carbonates sampled that were deposited during lake stages 1 and 3 contain *n*-alkanes in the range nC_{12}-nC_{29} (Table 3.2) with both bi-modal and uni-modal distributions. The thrombolite sample (3432.7 ft) exhibits an OEP of 1.49. The mudstone and marlstone samples deposited during lake stage 2 lack *n*-alkanes, with one exception of the mudstone at 3201.8 ft, which contains *n*-alkanes in the range of nC_{13}-nC_{22}. Samples from Douglas Pass (Table 3.2) are very lean, with no *n*-alkanes in the saturate fraction for any sample. *n*-alkanes are detected in both samples for core B824 (Piceance Basin) deposited during lake stage 3, and these span much shorter chain lengths nC_{13}-nC_{26} (Table 3.2). The *n*-alkanes for the microbial sample (fine-grained stromatolite) are bi-modally distributed, where the dolomitic oil shale has a uni-modal distribution lacking the presence of the higher chained *n*-alkanes >nC_{22}. The microbial sample for core B824 is heavily dominated by the lower chained-alkanes (nC_{13}-nC_{19}). The other core from Piceance Basin (E055, Table 3.2) has a wider distribution of *n*-alkanes (nC_{13}-nC_{29}). There is a marked change in the n-alkane distributions in the transition from lake stage 1 to 2. One sample (2709.8) a fine-grained stromatolite deposited during stage 1 of lake Uinta displaying an OEP of 1.50, similar to that of the thrombolite sample from well B987 also deposited during stage 1 of Lake Uinta.

The distribution of *n*-alkanes is bi-modal throughout this core, except for the two deepest samples, which are uni-modal. The two deepest samples (at 2535.5 ft. and 2709.8 ft.) are fine-grained stromatolites that were deposited during lake stage 1 and the majority of their *n*-alkane distributions are >nC_{21}.

Sample	*n*-alkanes	bimodal vs unimodal	OEP	TAR	Lake Stage
B987 3111	*n*-C_{12}-*n*-C_{28}	unimodal	nd	1.58	S3
B987 3201.8	*n*-C_{13}-*n*-C_{22}	unimodal	nd	nd	S2
B987 3202.7	nd	nd	nd	nd	S2
B987 3231.8	nd	nd	nd	nd	S2
B987 3397.4	nd	nd	nd	nd	S2
B987 3432.7	*n*-C_{14}-*n*-C_{21}	bi-modal	nd	nd	S1
B987 3437.9	*n*-C_{12}-*n*-C_{29}	bi-modal	1.49	14.80	S1
Douglas Pass Marlstone	nd	nd	nd	nd	S3
Douglas Pass Ooid Grainstone	nd	nd	nd	nd	S3
Douglas Pass Stromatolite	nd	nd	nd	nd	S3
B824 1363	*n*-C_{13}-*n*-C_{26}	bi-modal	nd	nd	S3
B824 1367	*n*-C_{13}-*n*-C_{25}	unimodal	nd	nd	S3
E055 1362.7	*n*-C_{15}-*n*-C_{29}	bi-modal	nd	1.20	S4
E055 1383.4	*n*-C_{13}-*n*-C_{28}	bi-modal	nd	0.53	S4
E055 1540.2	*n*-C_{15}-*n*-C_{28}	bi-modal	nd	0.74	S4
E055 1549.6	*n*-C_{16}-*n*-C_{28}	bi-modal	nd	0.54	S4
E055 1751.4	*n*-C_{13}-*n*-C_{26}	bi-modal	nd	0.31	S3
E055 1769.4	*n*-C_{17}-*n*-C_{27}	bi-modal	nd	0.47	S3
E055 1774.8	*n*-C_{15}-*n*-C_{28}	bi-modal	nd	0.91	S3
E055 2525.2	*n*-C_{14}-*n*-C_{27}	bi-modal	nd	0.83	S2
E055 2535.5	*n*-C_{14}-*n*-C_{28}	unimodal	nd	3.40	S2
E055 2709.8	*n*-C_{13}-*n*-C_{28}	unimodal	1.49	1.54	S1

Table 3.2: *N*-alkane distributions with calculated OEP and TAR ratios. Samples with no *n*-alkanes or higher chained *n*-alkanes were logged as "nd" meaning not determined. The odd-over-even predominance (OEP) is calculated by dividing the total peak area of the nC_{21}-nC_{27} odd *n*-alkanes by the total peak area of the nC_{22}-nC_{28} even *n*-alkanes. The terrigenous/aquatic ratio (TAR) is one means to quantify the relative inputs of marine algae and land plant sources, and is defined as: TAR = (*n*-C_{27} + *n*-C_{29} + *n*-C_{31})/(*n*-C_{15} + *n*-C_{17} + *n*-C_{19}) Samples are matched with their respective lake stage.

The ratio of Pristane (Pr)/Phytane (Ph) is representative of the preferential degradation of phytol in which oxic conditions promote a decarboxylation reaction to form Pristane and reducing conditions promote the formation of Phytane (ten Haven et al., 1987). Pr/Ph ratios that are >1 indicate oxic conditions of sedimentation (at the sediment/water interface), whereas values <1 reflect anoxic conditions (Didyk et al., 1978). Pristane/Phytane ratios in core B987 (Table 3.3) vary between 0.58 to 1.11. All samples are <1 except for the sample from 3432.7 ft. depth, which is >1 (1.1), and which was deposited in lake stage 1. No Pristane or Phytane compounds are identified in the Douglas Pass samples because no isoprenoids were preserved (Table 3.3). All ratios for core B824 (Table 3.3) are <1, and range from 0.58 to 0.84. Core E055 (Table 3.3) has very low Pristane/Phytane all <1, ranging from 0.13 to 0.44.

The relationship between the Pr/*n*-C_{17} and Ph/*n*-C_{18} biomarker parameters is related to the type (I, II, II/III) of kerogen in sedimentary organic matter (Obermajer et al. 1999). For core B987, Pr/*n*-C_{17} ranges from 0.23 to 1.38 and Ph/*n*-C_{18} ranges from 0.23 to 3.61 (Table 3.3). Douglas Pass samples have undetectable amounts of organic matter, so these ratios were not defined for those samples. The ratio of Pr/*n*-C_{17} in the core B824 samples ranges from 0.97 to 1.64 and Ph/*n*-C_{18} ranges from 1.13 to 3.12 (Table 3.3). For core E055, Pr/*n*-C_{17} ranges from 0.42 to 2.90 and Ph/*n*-C_{18} ranges from 2.30 to 17.19, a much wider distribution than any other core (Table 3.3).

Sample	Gammacerane Index	Isorenieratane	Pr/Ph	Pr/n-C_{17}	Ph/n-C_{18}	Lake Stage
B987 3111	1.18	nd	0.58	0.24	0.23	S3
B987 3201.8	1.72	nd	0.81	nd	nd	S2
B987 3202.7	0.91	nd	nd	nd	nd	S2
B987 3231.8	1.37	nd	nd	0.67	1.13	S2
B987 3397.4	0.71	nd	0.39	1.29	0.43	S2
B987 3432.7	1.65	nd	1.11	0.69	0.66	S1
B987 3437.9	0.54	nd	0.38	1.38	0.43	S1
Douglas Pass Marlstone	nd	nd	nd	nd	nd	S3
Douglas Pass Ooid Grainstone	nd	nd	nd	nd	nd	S3
Douglas Pass Stromatolite	nd	nd	nd	nd	nd	S3
B824 1363	0.94	nd	0.84	0.97	1.13	S3
B824 1367	2.07	nd	0.56	1.64	3.12	S3
E055 1362.7	0.89	nd	0.36	2.89	11.50	S4
E055 1383.4	1.35	nd	0.44	2.50	10.92	S4
E055 1540.2	0.86	nd	0.43	0.42	1.85	S4
E055 1549.6	0.91	nd	0.20	1.55	11.62	S4
E055 1751.4	nd	nd	0.39	0.87	3.71	S3
E055 1769.4	1.77	nd	0.22	0.71	5.62	S3
E055 1774.8	2.29	nd	0.13	0.59	17.19	S3
E055 2525.2	1.64	0.01	0.42	1.11	4.52	S2
E055 2535.5	0.28	nd	0.27	1.22	5.33	S2
E055 2709.8	0.51	nd	0.36	1.36	2.30	S1

Table 3.3: Pr/Ph, Pr/*n*-C_{17}, Ph/*n*-C_{18}, Isorenieratane and Gammacerane indexes. Gammacerane index is calculated using the equation 10xGammacerane/(Gammacerane + C_{30} Hopane). Gammacerane is present in all samples, which is indicative of water column stratification. All but one sample show Pr/Ph ratios <1 characteristic of a reducing anoxic environment. Samples are matched with their respective lake stage.

The *n*-alkane distributions for cores B987, B824, and E055 vary with the evolution of the lake, depositional environment and lithology. Lake stage 1 exhibits a dominant terrestrial organic matter signature while lake stages 2 and 3 have a decreased terrestrial influence and a more dominant algal signature. The microbialites and associated lithofacies

exhibit distinct distributions of *n*-alkanes from algal dominated to terrestrial dominated. The Pr/Ph ratios show evidence of anoxia with some oxidative turnover throughout the evolution of Lake Uinta. The ratios of Pr/*n*-C_{17} and Ph/*n*-C_{18} provide conclusions with regard to the type of kerogen present throughout each core.

3.3.2 Hopanes

Hopanes in these cores range from C_{29}-C_{31} with the dominant carbon chains being C_{29} and C_{30}. Ratios of C_{29}/C_{30} and C_{31}/C_{30} were calculated, as they represent industry standard in identifying source rocks (Peters et al., 2005b). C_{29}/C_{30} ratios >1 are characteristic of organic-rich carbonates and evaporites (Roushdy, et al., 2010). C_{31}/C_{30} ratios with values >0.25 indicate marine source rocks where values <0.25 are indicative of lacustrine source rocks (Peters et al., 2005b). No homohopanes (>C_{35}) are identified in any sample. For core B987 (Table 3.4), all samples have C_{29}/C_{30} ratios < 1 except a microbialite (a fine-grained stromatolite, 3111 ft. depth) with value 1.28. The C_{31}/C_{30} values for core B987 are all <0.25. There are no hopanes in the Douglas Pass samples (Table 3.4). For core B824 (Table 3.4), the values for C_{29}/C_{30} are <1 (0.57 and 0.15). As for C_{31}/C_{30} the values are <0.25. Core E055 has five samples with C_{29}/C_{30} ratios >1 and four with values <1 (Table 3.4). Three of the four with values >1 are microbial carbonates (stromatolites and thrombolites). In core E055, values for C_{31}/C_{30} are all <0.25, as in the other cores. Gammacerane, a C_{30} triterpane indicative of water column stratification, is in most samples (Tables 3.3). The abundances are calculated using the Gammacerane Index defined as (10 x Gammacerane/Gammacerane + C_{30} Hopane). There are no specified values in literature for the index, but increased water salinity is associated with higher Gammacerane Indexes >1 (Peters et al., 2005b). Gammacerane indexes are >1 for all samples in cores B987, B824 and

E055. No gammacerane is detected in the outcrop samples from Douglas Pass (Table 3.3). A diagenetic derivative of the carotenoid isorenieratane is identified in one sample from the E055 core from Piceance basin (Table 3.3).

Sample	C29 Hopane/C30 Hopane	C30 Hopane/C31 Hopane	C_{31}/C_{30}	Lake Stage
B987 3111	1.28	2.69	0.37	S3
B987 3201.8	0.52	1.00	1.00	S2
B987 3202.7	0.43	9.83	0.10	S2
B987 3231.8	0.15	4.21	0.24	S2
B987 3397.4	0.78	3.90	0.26	S2
B987 3432.7	0.11	5.58	0.18	S1
B987 3437.9	0.85	8.11	0.12	S1
Douglas Pass Marlstone	nd	nd	nd	S3
Douglas Pass Ooid Grainstone	nd	nd	nd	S3
Douglas Pass Stromatolite	nd	nd	nd	S3
B824 1363	0.57	4.44	0.23	S3
B824 1367	0.15	6.66	0.15	S3
E055 1362.7	0.74	7.27	0.14	S4
E055 1383.4	0.99	10.19	0.10	S4
E055 1540.2	1.61	6.53	0.15	S4
E055 1549.6	1.15	9.18	0.11	S4
E055 1751.4	nd	nd	nd	S3
E055 1769.4	1.17	6.79	0.15	S3
E055 1774.8	0.35	1.26	0.79	S3
E055 2525.2	1.15	8.30	0.12	S2
E055 2535.5	0.98	13.44	0.07	S2
E055 2709.8	1.48	3.72	0.03	S1

Table 3.4: Hopane ratios for all samples. Notice the abundance of the C_{30} homolog, relative to C_{29} and C_{31}. Samples are matched with their respective lake stage.

3.3.3 Steranes

Steranes C_{27}-C_{29} are identified in most samples, with the most abundant form being the C_{29} sterane. For B987, the least abundant homolog is C_{27}, which ranges from 0.05 to 0.27 %, and the C_{29} homolog, ranging from 0.35 to 0.70 % (Table 3.5). No steranes are

present in the extractable organic fraction for the Douglas Pass samples (Table 3.5). The C_{27} homolog is the least dominant compound in both Piceance cores as well, with values ranging from 0.06 to 0.27 % (Tables 3.5).

Sample	Sterane/Hopane	%C27 ST	%C28 ST	%C29 ST	C_{29}/C_{27} ST	Lake Stage
B987 3111	0.75	0.27	0.37	0.35	1.29	S3
B987 3201.8	nd	nd	nd	nd	nd	S2
B987 3202.7	0.84	0.06	0.24	0.70	10.97	S2
B987 3231.8	1.11	0.05	0.29	0.66	13.32	S2
B987 3397.4	0.35	0.27	0.27	0.46	1.67	S2
B987 3432.7	0.32	0.21	0.21	0.58	2.75	S1
B987 3437.9	0.94	0.19	0.19	0.63	3.37	S1
Douglas Pass Marlstone	nd	nd	nd	nd	nd	S3
Douglas Pass Ooid Grainstone	nd	nd	nd	nd	nd	S3
Douglas Pass Stromatolite	nd	nd	nd	nd	nd	S3
B824 1363	0.54	0.22	0.32	0.46	2.03	S3
B824 1367	0.45	0.13	0.30	0.57	4.28	S3
E055 1362.7	0.70	0.07	0.29	0.60	8.79	S4
E055 1383.4	1.11	0.11	0.43	0.47	4.27	S4
E055 1540.2	1.82	0.08	0.20	0.72	8.52	S4
E055 1549.6	0.63	0.13	0.21	0.66	5.01	S4
E055 1751.4	nd	0.20	0.36	0.44	2.16	S3
E055 1769.4	1.79	0.10	0.53	0.37	3.66	S3
E055 1774.8	1.28	0.27	0.42	0.31	1.13	S3
E055 2525.2	0.92	0.27	0.16	0.57	2.10	S2
E055 2535.5	1.25	0.24	0.21	0.55	2.30	S2
E055 2709.8	0.77	0.20	0.25	0.55	2.70	S1

Table 3.5: Sterane/Hopane ratio with Sterane percentages for each core and Douglas Pass outcrop samples. Notice the main sterane homolog for every sample is C_{29}. Samples are matched with their respective lake stage.

3.3.4 Polycyclic aromatic hydrocarbons (PAHs)

Polycyclic aromatic hydrocarbons (PAHs) are only found in B824 and E055, in the form of naphthalene (Table 3.6). To normalize for comparison between samples, the abundance of naphthalene is normalized to the abundance of phytane since phytane is

identified in every sample. B987 and Douglas Pass samples have undetectable amounts of aromatics (Table 3.6). For B824, the dolomitic oil shale contains aromatics in the form of naphthalene (Table 3.6). Aromatics are present in all but four samples in E055, with concentrations ranging from 0.007-0.05. Values are normalized to the abundances of phytane (Table 3.6).

Sample	PAH's	Lake Stage
B987 3111	nd	S3
B987 3201.8	nd	S2
B987 3202.7	nd	S2
B987 3231.8	nd	S2
B987 3397.4	nd	S2
B987 3432.7	nd	S1
B987 3437.9	nd	S1
Douglas Pass Marlstone	nd	S3
Douglas Pass Ooid Grainstone	nd	S3
Douglas Pass Stromatolite	nd	S3
B824 1363	0.04	S3
B824 1367	0.04	S3
E055 1362.7	0.05	S4
E055 1383.4	0.03	S4
E055 1540.2	nd	S4
E055 1549.6	0.04	S4
E055 1751.4	nd	S3
E055 1769.4	nd	S3
E055 1774.8	nd	S3
E055 2525.2	0.03	S2
E055 2535.5	0.01	S2
E055 2709.8	0.03	S1

Table 3.6: Aromatic compounds in samples collected. Notice that only cores B824 and E055 contained any aromatic compounds. Samples are matched with their respective lake stage.

CHAPTER FOUR: Discussion

4.1 Analysis of Extractable Organic Matter

An important piece to understanding these microbialites as reservoir and source rocks is assessment of the extractable organic matter distributions. The extractable organic matter distributions laid out in respect to the lake stages defined by Tänavsuu-Milkeviciene and Sarg (2012) help to establish the relationship between reservoir and source potential and depositional conditions in lacustrine systems.

4.1.1 N-alkane parameters

The use of *n*-alkanes to interpret organic matter source is based on the observation that short chain alkanes (*n*-C_{15} to *n*-C_{24}) are derived from marine algae and long chain alkanes (*n*-C_{25} to *n*-C_{31}) are derived from land plants (Peters et al., 2005b). The terrigenous/aquatic ratio (TAR) is one means to quantify the relative inputs of marine algae and land plant sources, and is defined as:

$$TAR = (n\text{-}C_{27} + n\text{-}C_{29} + n\text{-}C_{31})/(n\text{-}C_{15} + n\text{-}C_{17} + n\text{-}C_{19}).$$

This ratio is sensitive to other complicating factors, however: 1) thermal maturation and biodegradation (Peters et al., 2005b), and 2) land plant organic matter typically contains more *n*-alkanes than aquatic organic matter, which can lead to disproportionate weight assigned to land plant input (Peters et al., 2005b). Therefore, this ratio must be used in conjunction with other biomarker analysis (e.g., sterane distribution and sterane/hopane ratio) to accurately assess the source of organic matter. TAR ratios >1 indicate greater contributions by land plants than marine algae and values <1 indicate greater input from marine algae than from land plants (Peters et al., 2005b).

The *n*-alkane distributions for core B987 show evidence for both algal and terrestrial organic matter. TAR values for two microbialite samples from core B987 (Figure 4.1) (Table 3.2) range from 14.08 in a thrombolite (at 3437.9 ft. depth) deposited during lake stage 1 to 1.58 in a stromatolite (at 3111 ft. depth) deposited during lake stage 3, indicating the main biological source of the organic matter in these two samples is land plants. However, knowing that algal mats and cyanobacteria are primary constituents in the formation of microbialites (Riding, 2000) the algal and bacterial signature can't be overlooked. As mentioned above that TAR ratios can place disproportionate weight on the land plant contribution therefore sterane abundances and sterane/hopane ratios will be used to further assess the organic matter source.

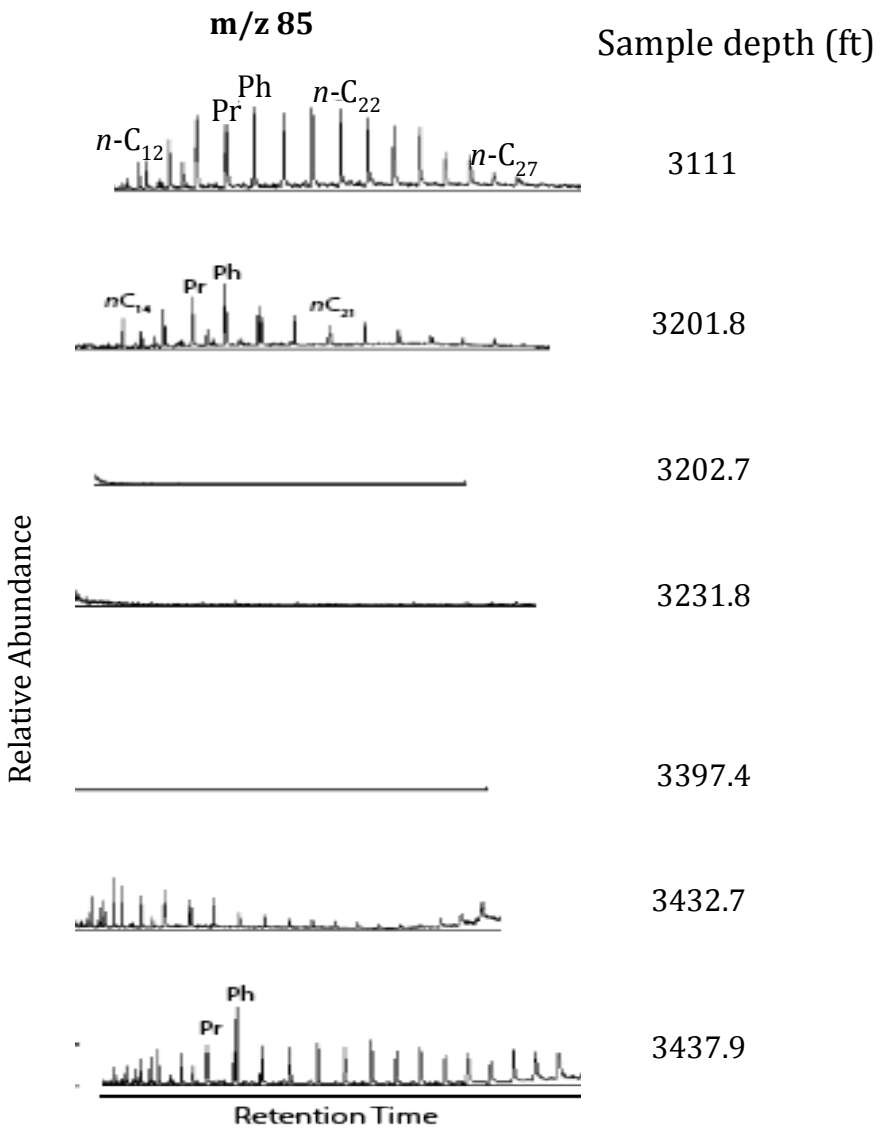

Figure 4.1: GC/MS mass chromatograms of m/z 85 the *n*-alkane distributions for core B987. Note the abundant *n*-alkanes in the fine-grained stromatolite at 3111 ft., the lack of *n*-alkanes transitioning to the deeper intervals, and distributions that transition from unimodal to bimodal with depth.

To further assess the controls on the source of organic matter to the Green River Formation the global climate reconstructions of Zachos et al. (2001, 2008) are referenced, which suggest that the Early Eocene was a period of sustained warming that peaked with the 2 myr long Early Eocene Climate Optimum (EECO) from 52 to 50 ma. This warming was

followed by a substantial cooling trend throughout the middle Eocene starting at 49 ma (Zachos et al., 2001, 2008). This warming trend at the beginning of the Eocene has been interpreted to align with lake stage 1 (Tänavsuu-Milkeviciene and Sarg, 2012), and which included abundant rainfall with runoff (Zachos et al., 2001). The thrombolites of lake stage 1 are intercalated with fluvial and deltaic deposits (Della Porta, 2013) that bring freshwater into the system along with land derived organic matter into the water column. The land derived organic matter is trapped on the accreting surface of the thrombolite explaining the evidence of TOM being so significant. The TOM signature isn't characteristic of the Green River microbialites, but with the abundant rainfall and land derived OM being transported into the lake margins during lake stage 1 it explains the signature in these microbialites. Also taking into account the disproportionate weight assigned to land plant OM in TAR ratios puts a better perspective on the source of OM in these microbialites. There is algal organic matter that is overshadowed by the land plant OM simply due to there being higher proportions of *n*-alkanes contained in land plant OM (Peters, et al., 2005b). However, the stromatolite from lake stage 1 doesn't include *n*-alkanes >nC_{21}. As mentioned earlier, *n*-alkanes are subject to biodegradation, and the lack of TOM can be attributed to bacterial degradation or aerobic degradation as a result of an influx of oxygen in the water column from runoff. The climate in lake stage 2 was dominantly arid with some seasonal flooding and runoff early in the stage (Tänavsuu-Milkeviciene and Sarg, 2012), interpreted from the core successions of heterogeneous deposits of siliciclastics in the form of deltaic sandstones. Towards the end of lake stage 2, the lake became more restricted (Tänavsuu-Milkeviciene and Sarg, 2012), accounting for the decrease in terrestrial organic matter. Three samples (one stromatolite, a mudstone and marlstone)

from this interval lack *n*-alkanes. This absence is interpreted to be a byproduct of seasonal flooding that brought oxygen into the water, and resulted in poor preservation of organic matter. The *n*-alkane distribution for a fourth sample (mudstone) deposited near the end of lake stage 2 exhibits a lack of TOM and a dominance of algal organic matter. This change may reflect the transition in Lake Uinta from a brackish lake to a restricted saline lake. The stromatolite sample from lake stage 3 (closed system, saline) shows an algal signature with an enriched land-derived *n*-alkane signature, which is interpreted to be due to degradation of the lower chained more labile compounds by bacteria. The general lack of an algal organic matter presence in the *n*-alkane distributions for core B987 indicates that conditions were not ideal for preservation of organics. Samples from the Douglas Pass outcrop had no detectable *n*-alkanes (Figure 4.2), which is a byproduct of oxidation of the organic matter due to the exposure of the outcrop.

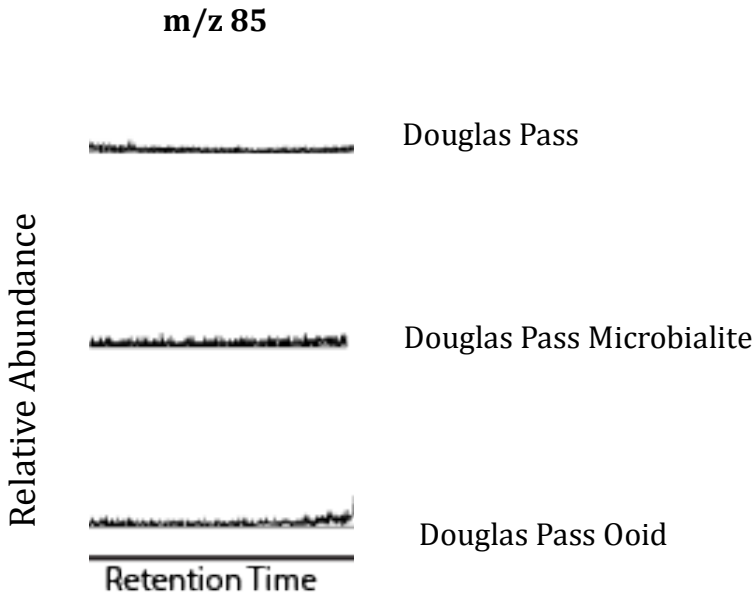

Figure 4.2: GC/MS mass chromatograms of m/z 85 the *n*-alkane distributions for the Douglas Pass samples. Note the lack of *n*-alkanes throughout all samples.

For core B824 (Figure 4.3) (Table 3.2), samples were gathered from strata deposited in lake stage 3. The TAR ratio is not calculated for either sample since the *n*-alkane distributions only range from *n*-C_{13} to *n*-C_{26}. However, the microbial sample displays a bimodal distribution of *n*-alkanes, with major sources of input from (1) algae and cyanobacteria and (2) archaebacteria. As for the dolomitic oil shale the *n*-alkane distribution is unimodal with a maxima at *n*-$C_{17,}$ indicative of an algal source. The predominant algal signature present in the *n*-alkane distributions suggests that the lake during stage 3 was anoxic with permanent water column stratification, which provided conditions ideal for the accumulation and preservation of organic matter.

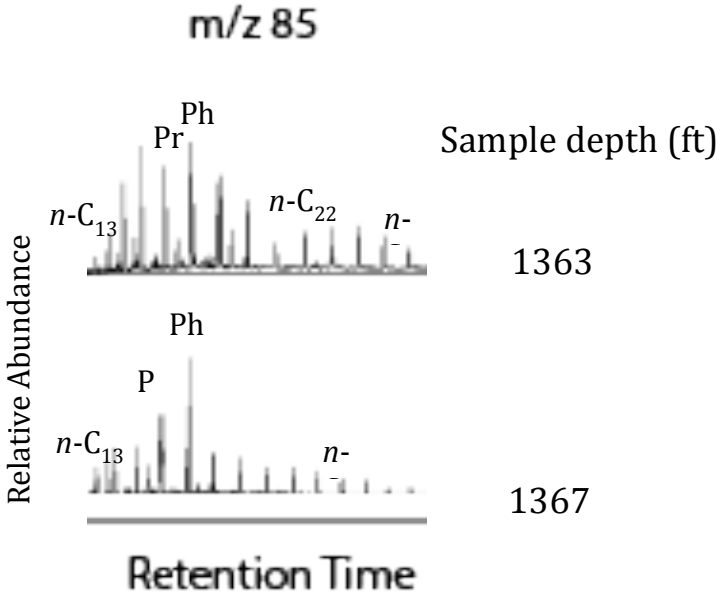

Figure 4.3: GC/MS mass chromatograms of m/z 85 the *n*-alkane distributions for core B824. Note the abundant *n*-alkanes with a bimodal distribution in the microbial sample at 1363 ft.

Overall, core E055 differs from core B987 with respect to *n*-alkane distributions, abundances and TAR ratios. TAR values for core E055 (Figure 4.4) (Table 3.2) range from 0.31 to 3.40. All but three of the samples have TAR values <1, indicating that the dominant source of organic matter is algae, aligning with the previous interpretations of Bradley (1931). Two samples (fine-grained stromatolite and thrombolite) with TAR values >1 were deposited in lake stages 1 and 2 (as with other samples with elevated TAR values in core B987), periods of abundant runoff and TOM input. The other sample with a TAR value >1 (siltstone) was deposited during the very beginning of lake stage 4, which was characterized by lake level rise and a cooling of the climate that brought an increase in precipitation. The initial cooling and increased precipitation brought more TOM into the basin as suggested by the *n*-alkane distributions. The three samples with TAR values >1 (fine-grained stromatolite, thrombolite and siltstone) are dominated by higher chained land plant derived *n*-alkanes, but still have algal-derived compounds. The remaining samples deposited in lake stages 2, 3, and 4 exhibit predominant algal signatures with TAR values <1, suggesting conditions in the lake were oxygen depleted, with little to no influence of aerobic bacterial degradation, and favoring preservation. The distribution of *n*-alkanes transitions in the microbialites from lake stage 1 at 2535.5 ft. and 2709.8 ft. from a more bimodal to uni-modal indicative of microbial degradation (Tissot et al., 1978). This degradation is interpreted to result in the depleted algal signature (C_{15}-C_{19}) of the *n*-alkanes in the three deepest samples. A byproduct of microbial degradation is an enhanced plant signature in the *n*-alkane distributions. The algal fraction is more labile and is more

easily degradable. The predominant algal signature in the *n*-alkanes is similar to the source rocks of the pre-salt, in Santos Basin, Brazil, which is dominated by *n*-alkanes ranging from *n*-C_{15}-*n*-C_{24} (Kuo, 1994).

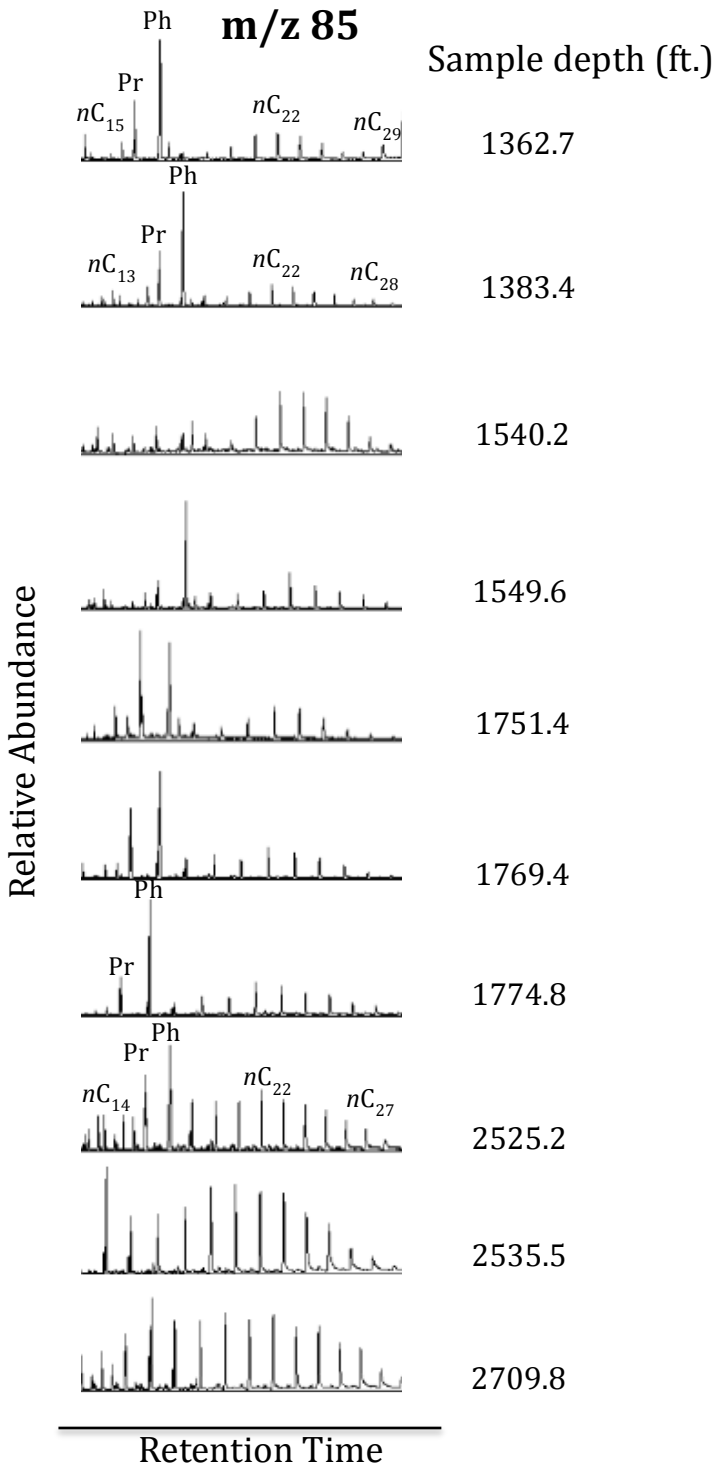

Figure 4.4: GC/MS mass chromatograms of m/z 85 the *n*-alkane distributions for core E055. Note the transition from bimodal to unimodal distributions with increasing depth.

4.1.2 Sterane Parameters

The application of the distribution of C_{27}, C_{28}, and C_{29} regular steranes in determining biological source of organic matter is based on the observation that steranes are derived from sterols found in most higher plants and algae, but are rare or absent in prokaryotic organisms (Waples, 1990). Sterane distributions for all cores (B987, B824, E055) (Figures 4.5, 4.6, 4.7) have C_{29} as the most abundant homolog. The C_{29} homolog has been interpreted to be solely representative of terrestrial organic matter. For samples that contain no evidence of TOM in the *n*-alkane distributions, the source of the C_{29} homolog cannot be accounted if it is derived only from terrigenous organic matter. However, previous studies on saline lakes (e.g., Boon et al., 1983; Matsumoto et al., 1982) revealed that cyanobacteria from mats and green algae can be major sources of the C_{29} sterane. Therefore, for the microbial samples, a level of C_{29} can be attributed to cyanobacteria from the microbial mat that acted as the accreting surface.

For the two microbial samples from core B987 with TAR values >1, the abundant C_{29} sterane can be attributed mainly to the terrestrial organic matter, with minimal input from the cyanobacteria of the microbial mat. The abundant C_{29} sterane for the associated lithofacies (mudstone, marlstone and fine-grained stromatolite) with no TOM input is derived from algal and cyanobacterial sources.

To summarize, C_{29} is the most abundant sterane in core B824, and with no TOM evident in the *n*-alkane distribution, the derivative must be algal in origin. The sources of the C_{29} sterane in core E055 vary among lake stages. The C_{29} sterane is derived from TOM

and cyanobacteria in the microbialites deposited during lake stage 1 and 2. In contrast, the stromatolites, mudstone and marlstone samples deposited during lake stage 3 include a dominant source of the C_{29} sterane homolog of algae, as indicated by the dominant algal signature in the *n*-alkanes. For the siltstone and oil shale samples deposited during lake stage 4, the most abundant sterane is the C_{29} homolog.

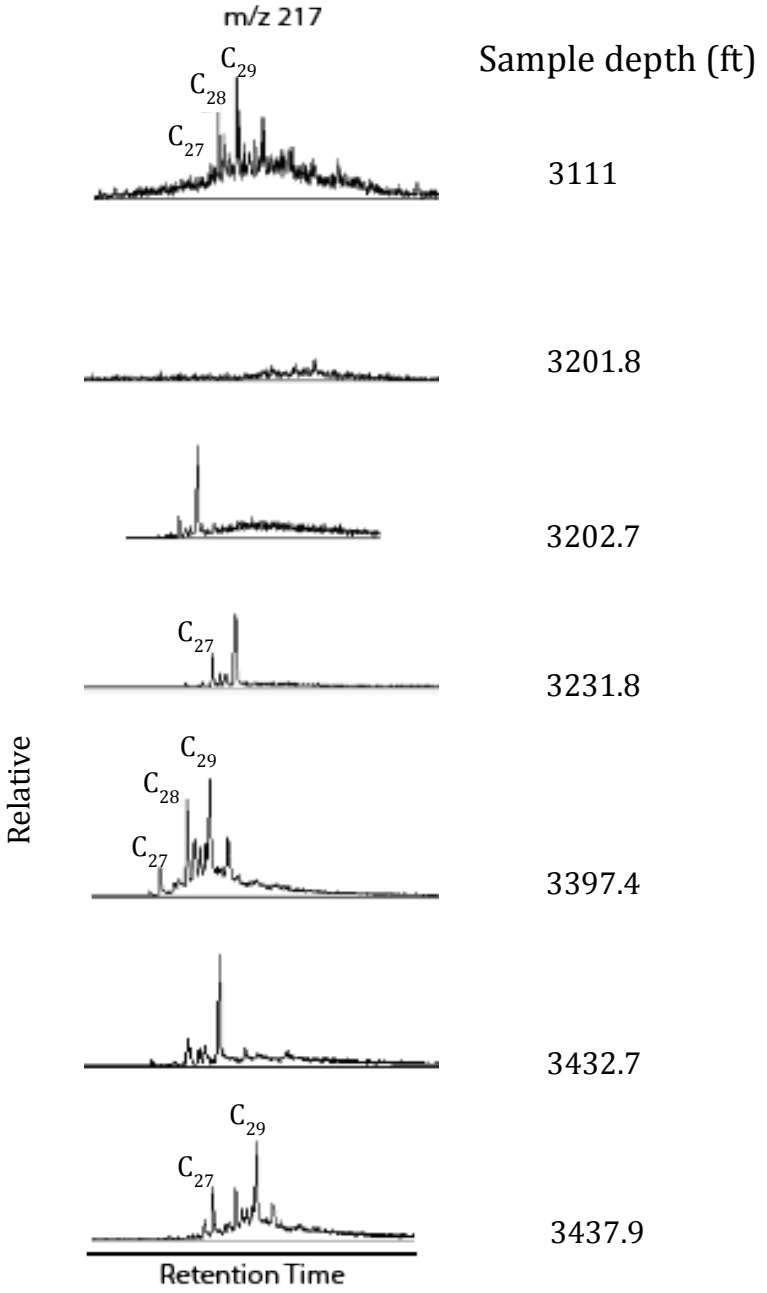

Figure 4.5: GC/MS mass chromatograms of m/z 217 the sterane distributions for core B987. The most abundant homolog present throughout the samples is C_{29}.

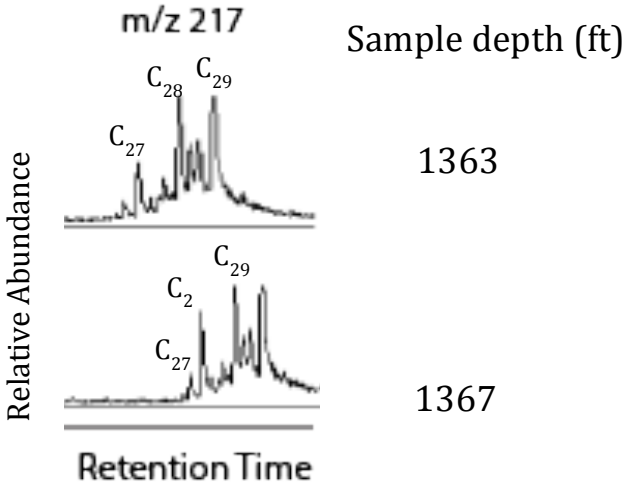

Figure 4.6: GC/MS mass chromatograms of m/z 217 the sterane distributions for core B824. The C_{29} homolog is the most abundant sterane in both samples.

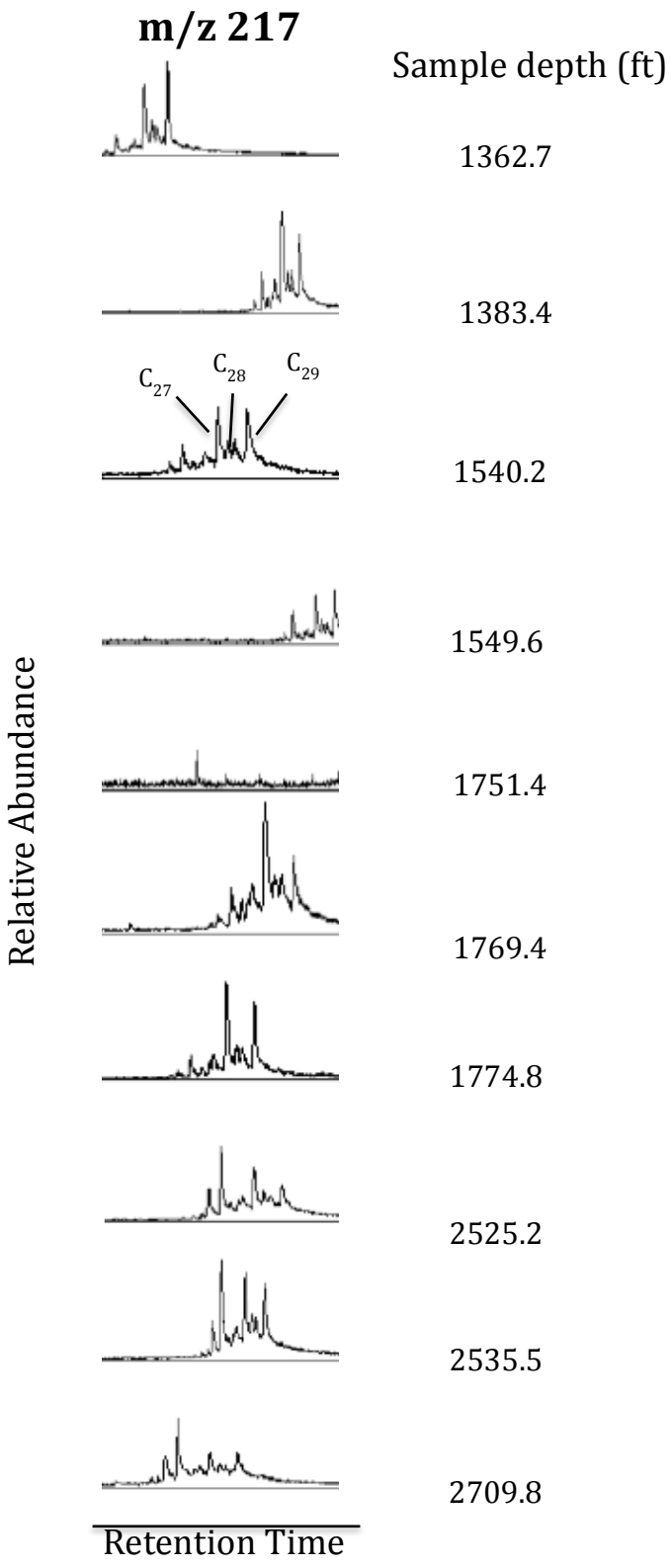

Figure 4.7: GC/MS mass chromatograms of m/z 217 the sterane distributions for core E055. Similar to cores B987 and B824 the most abundant sterane is in the form of C_{29}.

4.1.3 Sterane/Hopane parameter

The sterane/hopane ratios, which are used to indicate the ratio of prokaryotic versus eukaryotic input for a system, can be used to further asses the source of organic matter. For core B987 (Table 3.6) sterane/hopane values are indicative of a predominance of prokaryotic input. The dominant prokaryotic presence indicative of bacteria, which can cause degradation of OM helps to explain the lack of *n*-alkanes observed in the lake stage 1 microbialite samples, as well as the lake stage 2 mudstone and marlstone samples. Therefore, due to the algal fraction being more labile and easily degradable, it is preferentially degraded causing an enhanced TOM signature in the stage 1 and 3 microbialites. However, there is one exception, sample 3231.8, a marlstone dominated by eukaryotic input (algae), as indicated by the sterane/hopane ratio >1. As stated previously, the C_{29} homolog commonly is associated with terrestrial input, but can also be a byproduct of algae. The sterane/hopane ratio coupled with the *n*-alkane distributions, which lack evidence of TOM, confirms that the major organic matter source for the marlstone sample at 3231.8 ft is algal. Combining the results of the *n*-alkane distributions, sterane abundances and sterane/hopane ratios for core B987suggests that the dominant source of organic matter in core B987 is TOM, which can be further interpreted to reflect abundant rainfall and a high influx of runoff. With this interpretation, the combination of bacterial degradation and runoff during the rainy season limited the occurrence of algal activity as well as preservation. Low sterane/hopane ratios are a common feature associated with lacustrine sediments (Peters and Moldowan, 2005; Schiefelbein et al., 1999). These samples lack the C_{30} homolog, which is also indicative of lacustrine depositional environments (Holba et al., 2000).

The sterane/hopane ratios are between 0.45 and 0.54 for B824 (Table 3.6), which is indicative of lacustrine deposits, but interpreted to be representative of dominant prokaryotic input. However, both the *n*-alkane distributions and sterane abundances are inconsistent with this interpretation, and instead, are more indicative of algal input. For microbial samples, it is common to see low sterane/hopane values due to cyanobacterial input and microbial reworking of the organic matter (Tissot and Welte, 1984). For dolomitic oil shale, low sterane/hopane values are characteristic of lacustrine deposition, but also the *n*-alkane distribution that exhibits an archaebacterial signature, which contributes to abundances of hopanes. The values for C_{31}/C_{30} hopanes are 0.15 for the dolomitic oil shale and 0.23 for the fine-grained stromatolite, both of which are typical of lacustrine source rocks (Peters et al., 2005).

For core E055 (Table 3.6), the sterane/hopane ratios, which range from 0.63 to 1.82, indicate a mixture of eukaryotic and prokaryotic dominance throughout the samples. The thrombolite sample deposited during lake stage 1 has a sterane/hopane ratio <1 (0.77), which is usually associated with prokaryotic dominance, but can also be attributed to microbially reworked or terrigenous organic matter. In this case, biodegradation from prokaryotes (microbial communities) may enhance the TOM signature in the *n*-alkanes, causing both the high TAR value and low sterane/hopane ratio. The two fine-grained stromatolites deposited during lake stage 2 indicate a mixture of both prokaryotic and eukaryotic influence with ratios of 0.92 and 1.25. For sample 2525.2 the sterane/hopane ratio of 0.92 is indicative of terrigenous or microbially reworked organic matter. In this case combining the results of *n*-alkane distributions and sterane abundances, which indicate algal input, and the fact that microbes are key in the formation of microbialites

(Riding, 2006) it can be concluded that the low sterane/hopane abundance is due to microbial reworking. For sample 2535.5 the sterane/hopane ratio of 1.25 means that planktonic or benthic algae sourced the OM, but the TAR value contradicts this exhibiting a TOM signature. Again using caution when taking the TAR value into account, the *n*-alkane distributions and sterane data prove that there is significant cyanobacterial and algal input. With less organic matter contained in the algae and microbial degradation, TOM has a higher weight assigned to it, therefore the source can be resolved to being a mix of algal and TOM. The fine-grained stromatolites deposited in lake stage 3 have sterane/hopane ratios >1, indicative of algal organic matter, which is consistent with both the *n*-alkane and sterane abundance data. The algal content is much higher in the microbialites, which have microbial mats commonly algal in origin acting as the accreting surface in most stromatolites (Riding, 2000). The marlstone and mudstone samples of lake stage 3 exhibit strong prokaryotic signatures, although the *n*-alkane distributions (nC_{22}-nC_{24}) as well as sterane abundances (44-77% C_{29}) show algal dominance. The siltstone and oil shale samples of lake stage 4 have a mix of eukaryotic and prokaryotic input (1.11, 0.70), interpreted to represent climatic cooling and an increase in precipitation as indicated by the increased abundance of siliciclastic turbidites in core. The oil shale sample indicates algal organic matter input, which corresponds with the organic matter input exhibited by the TAR values and sterane abundances for that sample. The siltstone sample with a sterane/hopane ratio of 0.70 is interpreted to represent microbially reworked and terrigenous organic matter, as suggested by the TAR value of 1.20.

4.2 Pr/Ph

The ratio of Pristane to Phytane is an indicator of redox conditions in ancient sediment (Didyk et al., 1978). The most abundant source of Pristane (C_{19}) and Phytane (C_{20}) is the phytl side chain of chlorophyll a in phototrophic organisms and bacteriochlorophyll a and b in purple sulfur bacteria (e.g., Brooks et al., 1969; Powell and McKirdy, 1973). Reducing or anoxic conditions promote cleavage of the phytol side chain that ultimately reduces to Phytane. In contrast, oxic conditions favor the conversion of phytol to Pristane (Peters et al., 2005b). Low Pr/Ph ratios (<1) therefore occur in reducing or anoxic conditions, whereas values >1 are representative of oxic deposition. A special case in which there may be some application of the Pr/Ph ratio as an environmental indicator, are a hypersaline environments of deposition (ten Haven et al., 1987). The Pr/Ph ratio can be used because hypersaline environments can have high biological productivity with a very scarce diversity of organisms. However, halophilic bacteria are among the few organisms capable of thriving in a hypersaline environment and are known to contain complex lipids with a phytanyl moiety in much higher amounts than in methanogenic bacteria. These processes explain why sediment from hypersaline environments are characterized by particularly low Pr/Ph ratios (ten Haven et al., 1987).

In core B987, four of the five Pr/Ph ratios are <1 (Table 3.3), indicative of an anoxic environment with a period of oxidative conditions caused either by stream runoff introducing more oxygen into the water column or by seasonal turnover in the water column. The sample showing a Pr/Ph ratio >1 was deposited during lake stage 1, during which abundant rainfall and runoff may have brought oxygen into the deeper waters. For

the cores from Piceance Basin (B824, E055) (Table 3.3), the Pr/Ph values are all <1, indicating anoxia and hypersalinity throughout lakes stages 1, 2, 3, and 4.

The abundance of Gammacerane, a C_{30} triterpane commonly considered to be an indication of water column stratification, was measured relative to the abundance of C_{30} hopanes. Gammacerane indexes (Gammacerane/ (Gammacerane + C_{30}hopane)) for all samples are >1. The Gammacerane indexes being >1 indicate Lake Uinta was indeed a stratified lake.

4.3 Pr/n-C_{17} and Ph/n-C_{18}

n-alkane distributions, sterane abundances and sterane/hopane ratios suggest three possible sources of organic matter for the Green River samples: (1) aquatic algae, (2) organic material from terrestrial plants that was carried by the streams feeding the lake, or deposited by the wind, and (3) cyanobacteria and phytoplankton. The main biological source and redox conditions at time of sediment deposition can be inferred using log-log plots of the abundance of Pr/n-C_{17} versus Ph/n-C_{18} (Lijmbach, 1975). Also, the relationship between the Pr/*n*-C_{17} and Ph/*n*-C_{18} biomarkers is related to the type (I, II, II/III) of kerogen in sedimentary organic matter (Obermajer et al. 1999). Type I kerogen (oil-prone) is referred to as Sapropelic and it is made up of cyanobacteria, algae and derives mainly from lacustrine algae (Peters and Cassa, 1994). It forms primarily in lacustrine settings that are anoxic and provide ideal conditions for preservation of organic matter (Peters and Cassa, 1994). Type II kerogen (oil-prone) referred to as Planktonic is also dominated by lipid-rich algal and planktonic organic matter formed in lacustrine settings (Peters and Cassa, 1994). Type III (gas-prone) referred to as humic is formed from terrestrial organic matter (Peters

and Cassa, 1994). Type IV kerogen is "dead carbon" from which little to no hydrocarbons are produced during maturation (Peters and Cassa, 1994).

For core B987 (Figure 4.8), the crossplot (n=4) indicates the primary source of the sedimentary organic matter is Type II/III planktonic and terrestrial in origin and deposited in reducing conditions. One sample, a marlstone at 3231.8 ft., plots as Type I kerogen (algal in origin). The marlstone sample at 3231.8 ft. contained no TOM and exhibited a sterane/hopane ratio >1 and the most abundant sterane was C_{29}, consistent with the algal derived signature. The crossplot corresponds with the *n*-alkane distributions, sterane abundances, Pr/Ph ratios, and sterane/hopane ratios. The kerogen found in the pre-salt source rocks is primarily Type I and some Type II with TOC values ranging from 2-5% (Burwood et al., 1992). These samples from core B987 in Uinta basin both the stromatolites and thrombolites along with the marlstone and mudstone samples containing predominantly Type III kerogen and TOC values <1% do not have the same generative potential as the source rocks of the pre-salt.

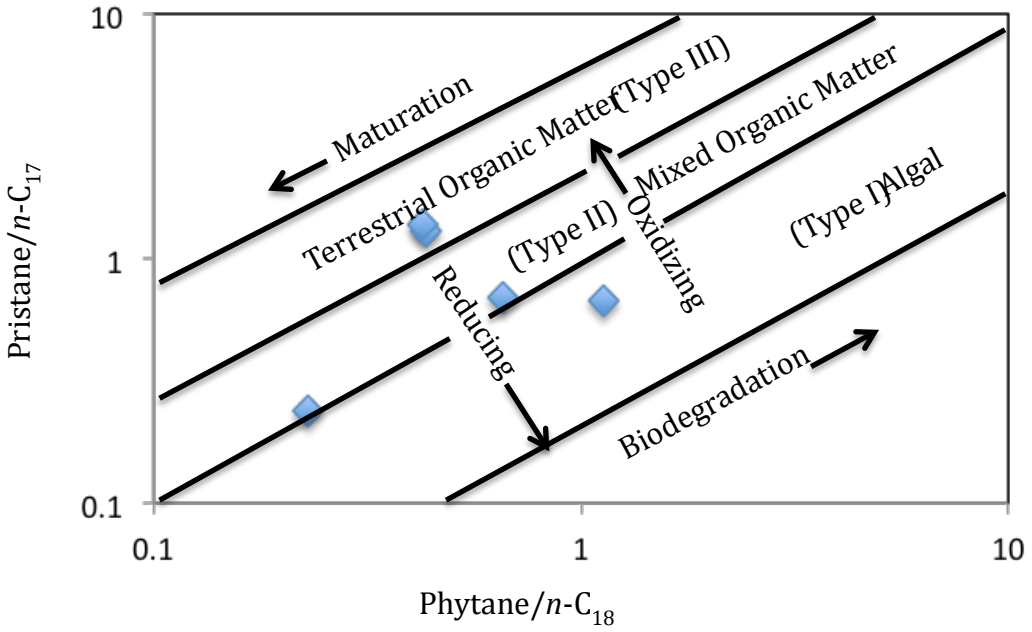

Figure 4.8: Pr/nC_{17} vs Ph/nC_{18} crossplot (Younes and Philip, 2005) for core B987 revealing mmature, biodegraded mixed and aquatic algae source . Note the dominance of mixed organic matter Type I and II with a dominance of terrestrial input, Type III.

For B824 (Figure 4.9), the crossplot (n=2) yields a dominantly algal contribution (Type I kerogen), deposited in a reducing environment, which corresponds with Pr/Ph ratios of <1. This result is similar to results of geochemical analysis on the pre-salt source that identified the main kerogen type in the source rocks as Type I of algal origin (Kuo, 1994). The crossplot (n=6) for E055 (Figure 4.10) revealed Type I kerogen (algal) deposited in reducing conditions, a type consistent with the source rocks of the pre-salt in Santos Basin, Brazil, Angola and Gabon (Kuo, 1994; and Pasley, 1998).

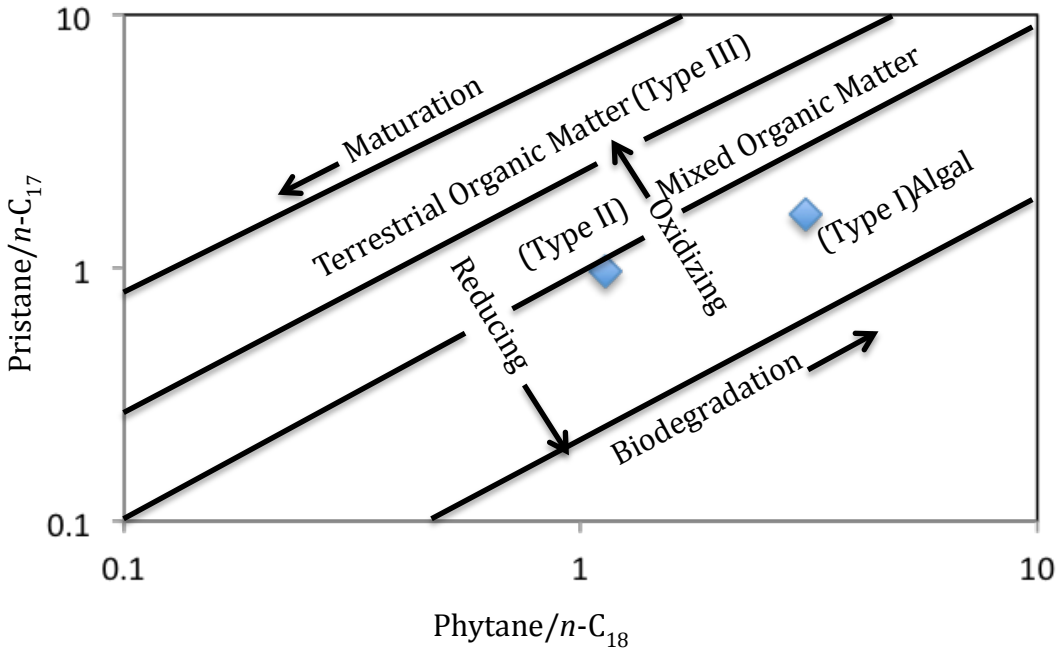

Figure 4.9: Pr/nC_{17} vs Ph/nC_{18} crossplot (Younes and Philip, 2005) for core B824illustrating immature, biodegraded aquatic algae source . The dominant form of kerogen in core B824 is Type I or algal in origin deposited in a reducing environment and was subject to biodegradation.

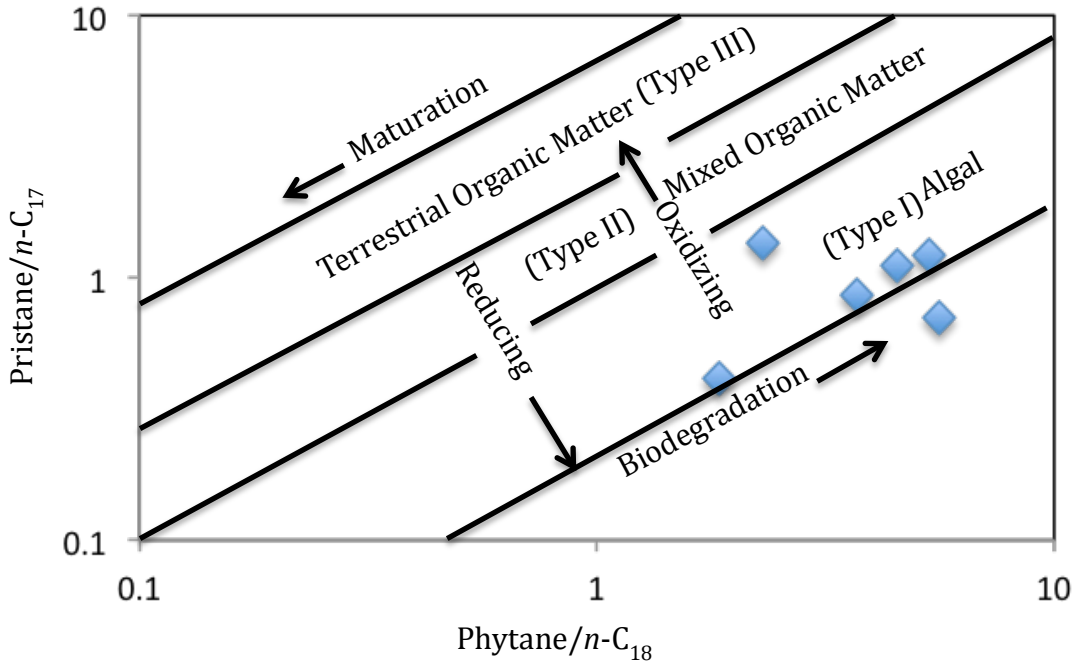

Figure 4.10: Pr/nC_{17} vs Ph/nC_{18} crossplot (Younes and Philip, 2005) for core E055suggesting an immature, biodegraded aquatic algae source. The samples of core E055 were deposited in a heavily reduced zone and were subject to biodegradation. All samples contained predominantly Type I kerogen (algal).

4.4 Depositional Model

The *n*-alkane distributions, Pr/Ph ratios, Gammacerane indexes, sterane abundances, and sterane/hopane ratios indicate the lake in the Uinta Basin was stratified with primarily anoxic conditions, although oxidative turnover may have occurred in the lake (based on the sample with a Pr/Ph ratio >1). These data are consistent with the interpretations of Boyer (1982) and Sullivan (1985) who suggested that a deep stratified lake and playa fringes could coexist.

The lake varied through time, however. Lake stage 1 was a time of warm climate with abundant rainfall resulting in abundant allochthonous terrestrial influx bringing

oxygen into the lake, causing oxidative turnovers and aerobic degradation of organic matter. Lake stage 2 was a drier, more seasonal climate, resulting in fluctuating lake levels and salinities. The abundant clastic dilution of organic matter during stage 2 was a product of increased seasonality and flash flood runoff, which in turn caused periodic increases in oxygen concentrations as indicated by the Pr/Ph values >1. Lake stage 3 is characterized by little to no TOM presence in the *n*-alkane distributions, Pr/Ph values <1, and Gammacerane indexes >1, all indicating the lake was anoxic and restricted with no influx of runoff. The factors favored development of a thermocline and a chemocline. This stage presents the most optimal conditions for preservation of organic matter, especially the more labile algal compounds. The *n*-alkane distributions, Pr/Ph ratios, Gammacerane indexes, sterane abundances, and sterane/hopane ratios indicate the lake in the Piceance Basin was stratified with anoxic bottom waters with minor TOM input, but overall a dominant algal signature in the organic matter. Evidence of terrestrial organic matter is present mainly in the microbialite samples, due to the trapping and binding of grains onto the microbial mat acting as the accreting surface. The samples in which TOM is present it accounts for 25-30% of the organic matter. With the microbial mat being composed primarily of cyanobacteria and algal components the presence of TOM is indicative of the incorporation of allochthonous organic matter into the growing microbialite (Arp et al., 1999). Samples from cores E055 and B824, deposited during Lake Uinta stage 3 exhibit very low Pr/Ph values, Gammacerane indexes >1, and abundant *n*-alkanes, confirming this stage to include anoxia and hypersalinity. From stage 2 to stage 3, there was a climactic shift from humid to more arid, as suggested by the decrease in TOM signatures in the *n*-alkane distributions that caused the lake level to fluctuate due to evaporation exceeding the run-off from

streams. This change is interpreted to have been accompanied by a decrease of siliciclastics and deposition of nahcolite beds within upper lake stage 3 strata (Roehler, 1974). The lake during stage 3 also became more restricted, as suggested by the *n*-alkane distributions, Pr/Ph ratios, Gammacerane indexes and sterane/hopane ratios, which suggest a stratified water column with anoxic waters that preserved organic matter. Transitioning into lake stage 4, the climate began to cool, and rainfall began to increase. These changes in climate were marked depositionally by the sandstones with load and flame structures consistent with turbidites, which indicate runoff from storms or periods of intense rainfall. The lake however, remained stratified and anoxic as indicated in the Pr/Ph ratios and Gammacerane indexes. Lake stage 5 is characterized by the maximum lake level reached in the evolution of lake Uinta, where thick oil shales were deposited in an anoxic stratified lake. There are no microbialite deposits present in lake stage 5, so no samples were gathered from this interval. No microbialites were deposited during lake stage 6 either, which marked the closing of the lake, with an increasing abundance of turbidite deposits and volcaniclastic sediments.

4.5 TOC and Source Rock Properties

Overall, the microbialites are more organic rich than the surrounding mudstones, marlstones, oil shales, peloidal wackestones to packstones, and oolitic grainstones. Additionally, geochemistry illustrates dissimilarities among the microbialites, mudstones, oolitic grainstones, dolomitic marlstones and peloidal wackestones/packstones in reference to the reservoir and source potential of these rocks.

TOC is a common geochemical measure used to evaluate the organic richness of a rock, including unconventional reservoirs. Shale or carbonate rocks with TOC values between 1-2 wt. % are considered by Peters et al., (1986) to have sufficient organic richness to act as source rocks, and TOC values >2.0% are considered excellent source rocks with the greatest potential to yield hydrocarbons (Peters, 1986). In particular, the Upper Barremian Coquinas Sequence composed of alternating carbonate (microbial grainstones, wackestones, and coquinas) and shale beds are responsible for contributing the majority of the hydrocarbons discovered in the Campos Basin (Trindade et al., 1995). The TOC values for the Upper Barremian Couquinas Sequence range from 2-12% (Trindade et al., 1995).

TOC in core B987 (Table 3.1) from Uinta Basin ranges from 0.14 to 1.7 % with the highest value in microbialite. The interval sampled for this core is within the Douglas Creek Member, which represents lake stages 1, 2, and 3 of lake Uinta. Overall, samples in this core are not source quality rocks based on average measured TOC values of <1%. The TOC values of samples for core B987 both microbial boundstones (stromatolites and thrombolites) and associated mudstone and marlstones are not consistent with those of the pre-salt source rocks.

For core B824 (Table 3.1), only two samples were collected, one fine-grained stromatolite and dolomitic oil shale. The TOC values for this core are elevated drastically compared to the samples from Uinta basin. Measured TOC ranges 29.27% for the associated lacustrine carbonate to 39.71% for the microbialite. These samples are from the Parachute Creek Member, deposited during lake stage 3, a period of high amplitude fluctuations in water depths with high organic richness due to anoxic bottom waters.

Based on TOC measurements, both the microbialite and associated lacustrine carbonate are potential source rocks.

For core E055 (Table 3.1), TOC values range from 4.52% to 28.89%, all in the range of organic-rich source rocks (as defined by Peters, 1986). Lake Uinta in Piceance Basin was a hydrologically closed, hypersaline anoxic lake, similar to the pre-salt deposits (Nombo-Myaka and Hong Han, 2009) which show analogous organic richness. The strata sampled for this core span the Garden Gulch and Parachute Creek members deposited in lake stages 1, 2, 3, and 4. The lake in Piceance Basin was geochemically independent of the lake in Uinta Basin, as suggested by the differing stratal packages along with differences in the *n*-alkane distributions, sterane abundances, sterane/hopane ratios, Pr/Ph ratios, and TOC measurements. Core B987 (Uinta Basin) exhibited much more abundant siliciclastic deposition with higher TOM input, periods of oxidative turnover and significant biodegradation of the *n*-alkane fractions. On the other hand, cores B824 and E055 (Piceance Basin) contained much less siliciclastic deposition, dominant algal organic matter input, water column stratification throughout, with anoxic conditions optimal for organic matter preservation.

Based on the bulk geochemistry (TOC), no clear distinction can be made between the microbialites and associated lithofacies establishing one or the other as the better source rock. However, elevated TOC is necessary, but not sufficient, to document the source potential of a rock. There also has to be a substantial amount of hydrogen present in the organic matter to make hydrocarbon compounds (Peters and Cassa, 1994). The type, source, and quantity of organic matter, in addition to overall organic richness, are key standards that can determine source potential.

4.6 Reservoir and Source Potential

To accurately predict the reservoir and source potential of these rocks, the type, source, and relative abundances of the extractable organic matter and the TOC data must be assessed. Relative abundances of the saturated and aromatic fractions indicate that the microbial carbonates (fine-grained stromatolites and thrombolites) have greater potential to act as reservoir and source than the associated marlstone, ooid grainstone, mudstone, and oil shales. The relative abundances of the saturated fractions for the microbial samples in cores B987, B824 and E055 are orders of magnitude (10x and 100x) greater than those of the associated oolitic grainstone, dolomitic marlstone, and mudstone (Figure 4.11). Although there is a measurable difference between the abundances of the saturated and aromatic fractions in core B987 for the fine-grained stromatolite and mudstone, $6.00x10^6$ and $6.00x10^5$, respectively, the TOC values are all 1% or below, indicating these deposits are very lean.

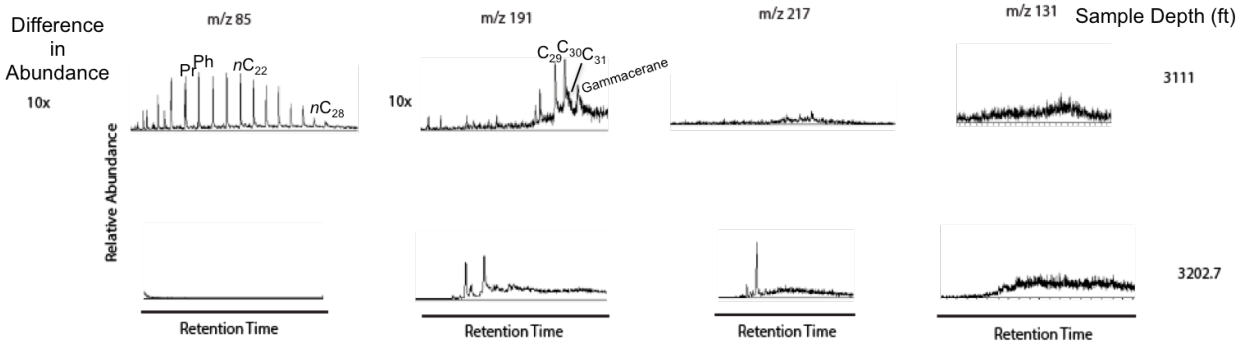

Figure 4.11: GC/MS mass chromatograms of the saturated and aromatic hydrocarbon fractions for a fine-grained stromatolite (3111 ft.) deposited in lake stage 3 and a mudstone (3202.7 ft.) from lake stage 2 of core B987. Note the abundances of the saturated and aromatic fractions in the microbial sample are 10x greater than the mudstone.

From a source rock perspective, the mudstone, marlstone, or microbialites of core B987 have no potential to produce hydrocarbons. However, the microbialite from lake

stage 3 (3111 ft.) has a TOC wt% of 1.7% with similar OM sources (Type II and III kerogen) to oils being produced within the basin. The wt % TOC is too lean to classify this facies as a viable source rock, however, with similar OM to the oil in a field to south within the basin suggests that the microbialites can act as migration pathways and reservoirs. This field, the West Willow Creek Field in the Uinta basin, has a stromatolitic mound reservoir, where the source of the oil is from interbedded algal coals and oil shales (Osmond, 2000). The source rocks for West Willow Creek Field contain predominantly Type I organic kerogen, but some oil shales have Type III gas-prone kerogen (Mueller, 1998). The fact that the extractable organic matter of the microbialites has characteristics similar to that of the oil being produced from similar lithofacies within a similar stratigraphic succession in the same basin suggests these rocks have potential to act as petroleum reservoirs.

The Piceance basin is one of the largest oil shale deposits in the world (Johnson et al., 2010). Until the recent heightened interest in lacustrine systems with specific interest in lacustrine microbialites, “oil shale” was the only target for oil and gas production. Geochemical analysis proves the microbialites in Piceance basin to be more organic rich than the marlstone, mudstone and oil shale, with potential to act as both reservoir and source rocks. Although all samples in cores E055 and B824 are organic rich, there are orders of magnitude difference (10x and 100x) in the abundances of saturated and aromatic hydrocarbon fractions among the marlstone, mudstone, oil shale and microbial samples (Figure 4.12). A more complete interpretation of source potential can be derived from the crossplots of Pr/nC_{17} and Ph/nC_{18}, which show the predominant organic matter type is algal (Type I) for the Piceance Basin. The biomarker and TOC data suggest that the microbialites of the Piceance Basin have the greatest potential to yield hydrocarbons. In

fact, there is potential throughout the sample suite, but the "oil shale" of the Piceance Basin had already been labeled as a main source rock in previous studies whereas the microbialites had yet to be analyzed with respect to source and reservoir quality. Comparing the microbialites for both basins, the microbialites of Piceance basin exhibit relative abundances of the saturated and aromatic fractions 100x those of the Uinta basin microbialites. The discovered potential in microbialites provides new direction for studying these deposits, not only in the Green River Formation, but worldwide in the search for a greater understanding of lacustrine system.

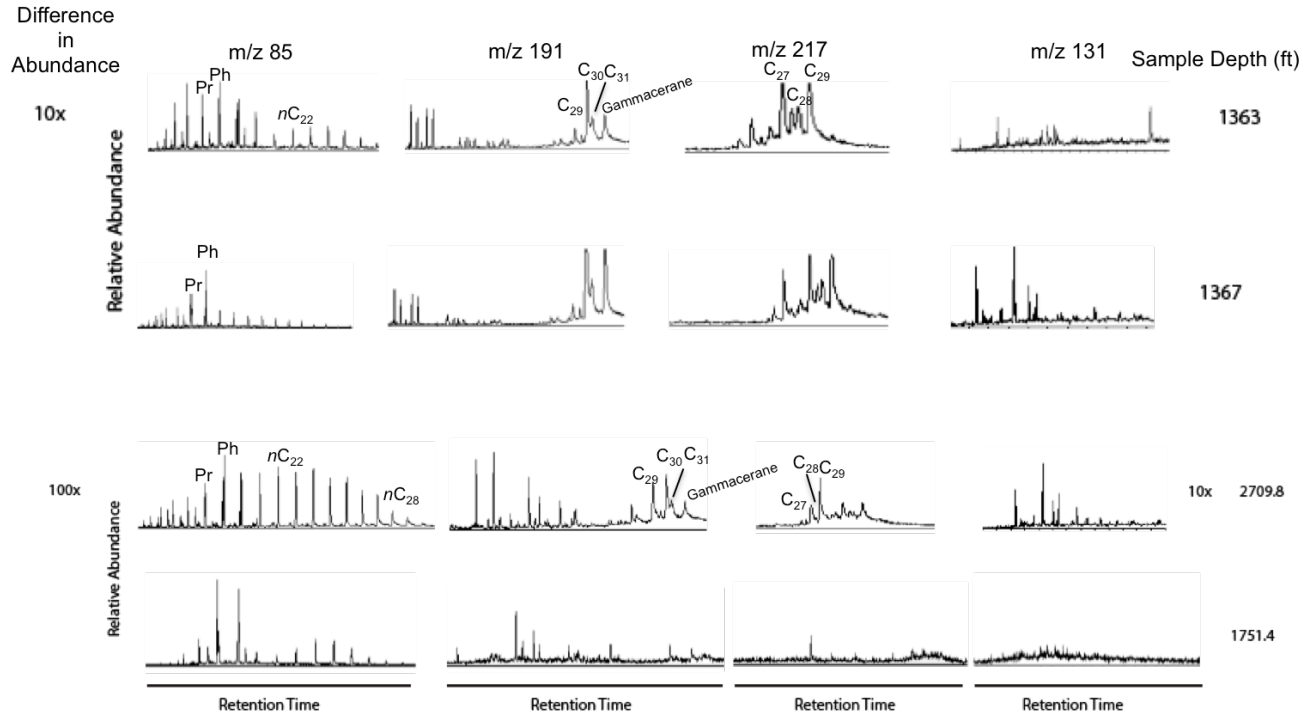

Figure 4.12: GC/MS mass chromatograms of the saturated and aromatic hydrocarbon fractions for cores B824 and E055. For core B824 both samples are from lake stage 3, however, the abundances of the microbial sample at 1363 ft are 10x greater than those of the dolomitic oil shale at 1367 ft. Note for core E055 the abundances of a thrombolite from lake stage 1 and evaporite from lake stage 3 have the greatest contrast at 100x more abundant in the microbial sample compared to the mudstone.

4.7 Implications for Lacustrine Systems Worldwide

Lacustrine systems are dynamic response systems that integrate environmental, climactic and tectonic forgings into a continuous, high-resolution archive of local and regional change (GIerlowski-Kordesch and Kelts, 2000) (Schnurrenberger, et al., 2002). Lacustrine systems have been known to hold prolific hydrocarbon reserves, more than 120 x 10^9 barrels of oil equivalent to be exact (Bohacs, 2012). As lakes are susceptible to varying changes during their evolution it makes it very tough to assess the reservoir and source potential of these systems. The organic matter found in lake sediments can be attributed to algae and plant debris, with the climate during lake evolution having direct influence on the type and abundance of organic matter preserved in lacustrine systems. Lacustrine systems experience differing sedimentation rates, and organic matter preservation as a function of climate (Virgone, 2013) and therefore vary in reservoir and source potential. Carbonate lacustrine systems contain good source rock prospects that occur in the deeper stratified lakes, where anoxic bottom waters and low detrital input permit the deposition and preservation of organic rich deposits (Platt and Wright, 1991). Lacustrine stromatolites similar to those present in the Green River Formation have been described in the Late Archean Meentheena Member of Austrailia, the Plio-Pleistocene of the East African Rift (Casanova, 1986), the Triassic of Greenland (Clemmensen, 1978), the Oligocene of southern France (Casanova and Nury, 1989), and the Tertiary of southern France (Truc, 1978) (Platt and Wright, 1991). While these stromatolites are similar in morphology and distribution they were deposited in unique lacustrine systems with varying climates, shoreline evolutions, sedimentation rates, and water chemistries thus affecting their organic matter distributions. With this study, we learn that lacustrine

systems can contain multiple source quality facies and with geochemical analysis it can provide insight into which facies prove to better source rocks and reservoir rocks. Assessing the organic matter distributions and TOC values for microbialites of ancient lacustrine systems, as a function of depositional environment will aid in lacustrine exploration. Understanding the genetic aspects of OM with lake evolution is a technique that can be applied to all lacustrine systems worldwide to predict the generative potential and reservoir distribution within the system.

CHAPTER FIVE: Conclusion

A study of the extractable organic material, bulk geochemistry suggests that the microbial carbonates of the Green River Formation have potential to act as both petroleum source and reservoir rocks. *n*-alkane distributions, sterane abundances, sterane/hopane ratios and Pr/*n*-C_{17} vs Ph/*n*-C_{18} crossplots from the Garden Gulch, Parachute Creek and Douglas Creek members of the Green River Formation are indicative of three main biological sources: (1) aquatic algae (interpreted to have formed during the more humid climate); (2) cyanobacteria; and (3) terrestrial organic matter that were transported via streams. The types, abundances, and distributions of preserved organic matter vary among the microbial carbonates and associated marlstone, mudstone, dolomitic oil shale, oolitic grainstone, and peloidal wackestone/packstones. These distributions are interpreted to vary as a function of climate, depositional environment, and rate of sediment influx. Core B987 was deposited near the lake margin where there was abundant siliciclastic input causing dilution of the organic matter and consists of predominantly Type III (terrestrial) kerogen. The microbialite samples contain greater abundances of organic matter than the

associated mudstones and marlstones, $6.0x10^6$ %/cm^3 and $6.0x10^5$ %/cm^3 respectively. Cores B824 and E055 were deposited near the depocenter where the anoxic conditions and limited siliciclastic input lead to organic rich deposits, where the dominant organic matter type is algal or Type I kerogen. The Type I kerogen for cores E055 and B824 is more oil prone and more organic rich than the Type III kerogen, which core B987 is predominantly composed of. The abundances of saturated and aromatic fractions are much greater in the microbialites than the surrounding mudstones, marlstones, and dolomitic oil shales; $3.0x10^9$ %/cm^3 and $7.0x10^7$ %/cm^3 respectively. The bulk geochemical data (TOC) suggests that core B987 is not of source rock quality, whereas cores B824 and E055 have source potential with TOC values >5% up to 39.71%. Understanding the types, abundances, and distributions of preserved organic matter in these rocks as a function of depositional processes is vital for providing a predicative framework for analyzing the source and reservoir potential and distribution of microbialite reservoirs within similar systems.

References

Aitken, J.D., 1967, Classification and Environmental Significance of Cryptalgal Limestones and Dolomites, with Illustrations from the Cambrian and Ordovician of Southwestern Alberta: Journal of Sedimentary Petrology, v. 37, no. 4, p. 1163-1178.

Awramik, S.M., and Sprinkle, J., 1999, Proterozoic Stromatolites: The First Marine Evolutionary Biota: Historical Biology, v. 13, p. 241–253.

Awramik, S.M., 1971, Precambrian Columnar Stromatolite Diversity: Reflection of Metazoan Appearance: Science, v. 174, p. 825-827.

Awramik, S.M., 1982, Precambrian Columnar Stromatolite Diversity: Reflection of Metazoan Appearance: Science, v. 216, p. 171–173.

Awramik, S.M., 1992, The History and Significance of Stromatolites, *in* Early Organic Evolution: Implications for Energy and Mineral Resources, Edited by: Schidlowski, M., Kimberley, M.M., McKirdy, D.M., Trudinger, P.A., Springer Berlin, p. 435-449.

Awramik, S.M., and Buchheim, H.P., 2012, The Quest for Microbialite Analogs to the South Atlantic Pre-Salt Carbonate Hydrocarbon Reservoirs of Africa and South America, paper presented during Houston Geological Society Joint General and International Dinner Meeting, September 10, p. 23–26.

Bohacs, K.M., Lamb-Wozniak, K., Demko, T.M., Eleson, J., McLaughlin, O., Lash, C., Cleveland, D.M., and Kaczmarek, S., 2013, Vertical and Lateral Distribution of Lacustrine Carbonate Lithofacies at the Parasequence Scale in the Miocene Hot Spring Limestone, Idaho: An Analog Addressing Reservoir Presence and Quality: AAPG Bulletin, v. 97, no. 11, p. 1967–1995.

Boyer, B.W., 1982, Green River Laminites: Does the Playa-Lake Model Really Invalidate the Stratified-Lake Model?: Geology, v. 10, no. 6, p. 321-324.

Bradley, W.H., 1964, Geology of the Green River Formation and Associated Eocene Rocks in Southwestern Wyoming and Adjacent Parts of Colorado and Utah: U.S. Geologic Survey Professional Paper 496-A, 86 p.

Bradley, W.H., and Eugster, H.P., 1969, Geochemistry and Paleolimnology of the Trona Deposits and Associated Authigenic Minerals of the Green River Formation of Wyoming: US Geological Survey Professional Paper 496-B, p. 71.

Brooks, J.D., Gould, K., and Smith, J.W., 1969, Isoprenoid Hydrocarbons in Coal and Petroleum: Nature, v. 222, p. 257-259.

Buchheim, H.P., Awramik, S.M., Leggitt, V.L., Demko, T.M., Wozniak, K.L., and Bohacs, K.M., 2012, Large Lacustrine Microbialite Bioherms from the Eocene Green River Formation: Stratigraphic Architecture, Sequence Stratigraphic Relations, and Depositional Model, paper presented at AAPG Hedberg Conference held in Houston, Texas, June 4-8, p. 1-2.

Buick, R., Dunlop, J.S.R., and Groves, D.I., 1981, Stromatolite Recognition in Ancient Rocks: An Appraisal of Irregular Laminated Structures in Early Archean Chert-Barite Unit from North Pole, Western Australia: Alcheringa, v. 5, p.161-181.

Burwood, R., Cornet, P.J., Jacobs, L., and Paulet, J., 1990, Organofacies Variation Control on Hydrocarbon Generation: A Lower Congo Coastal Basin (Angola) Case History: Organic Geochemistry, v. 16, no. 1, p. 325-338.

Carroll, A., Chetel, L.M. and Smith, M.E., 2006, Feast to Famine: Sediment Supply Control on Laramide Basin Fill: Geology, v. 34, no. 3, p. 197–200.

Carroll, A.R., and Bohacs, K.M., 1999, Stratigraphic Classification of Ancient Lakes: Balancing Tectonic and Climatic Controls: Geology, v. 27, no. 2, p. 99–102.

Cole, R.D., and Picard, M.D., 1978, Comparative Mineralogy of Nearshore and Offshore Lacustrine Lithofacies, Parachute Creek Member of the Green River Formation, Piceance Creek Basin, Colorado, and Eastern Uinta Basin, Utah: Geological Society of America Bulletin, v. 89, no. 10, p. 441-454.

Cole, R.D., 1985, Depositional Environments of Oil Shale in the Green River Formation, Douglas Creek Arch, Colorado and Utah: Geology and Energy Resources, Uinta Basin of Utah: Utah Geological Association Publication, v. 12, p. 211–224.

Colombo, J.C., Pelletier, E., Brochu, C., Khalll, M., 1989, Determination of Hydrocarbon Sources Using n-Alkane and Polyaromatic Hydrocarbon Distribution Indexes, Case Study: Rio de La Plata Estuary, Argentina: Environmental Science Technology, v. 23, p. 888-894.

Dean, W.E., and Anders, D.E., 1991, Effects of Source, Depositional Environment, and Diagenesis on Characteristics of Organic Matter in Oil Shale from the Green River Formation, Wyoming, Utah, and Colorado, *in* Geochemical, Biogeochemical, and Sedimentological Studies of the Green River Formation, Wyoming, Utah, and Colorado, Edited by Tuttle, M.L., U.S. Geological Survey Bulletin, ch. F, 143 p.

Desborough, G. A., and Pitman, J. K., 1974, Significance of Applied Mineralogy to Oil Shale in the Upper Part of the Parachute Creek Member of the Green River Formation, Piceance Creek basin, Colorado, *in* Rocky Mountain Association of Geologists Guidebook to the Energy Resources of the Piceance Creek basin, Colorado, 25th Field Conference, Edited by Murray, D.K., p. 81-89.

Desborough, G.A., 1978, A Biogenic-Chemical Stratified Lake Model for the Origin of Oil Shale of the Green River Formation: An Alternative to the Playa-Lake Model, Geological Society of America Bulletin, v. 89, no. 7, p. 961-971.

Didyk, B.M., Simoneit, B.R.T., Brassel, S.C., and Eglinton, G., 1978, Organic Geochemical Indicators of Palaeoenvironmental Conditions of Sedimentation: Nature, v. 272, p. 216-222.

Donnell, J.R., 1965, Geology and Oil-Shale Resources of the Green River Formation: The Mountain Geologist, v. 2, no. 3, p. 95–100.

Dupraz, C., Reid, R.P., Braissant, O., Decho, A.W., Norman, R.S., and Visscher, P.T., 2009, Processes of Carbonate Precipitation in Modern Microbial Mats: Earth Science Reviews, v. 96, no. 3, p. 141-162.

Eglinton, G., Hamilton, R.J., Raphael, R.A., and Gonzalez, A.G., 1962, Hydrocarbon Constituents of the Wax Coatings of Plant Leaves: A Taxonomic Survey: Nature, v. 193, p. 739-742.

Eugster, H.P., 1967, Hydrous Sodium Silicates from Lake Magadi, Kenya, Precursors of Bedded Chert: Science, v. 157, no. 3793, p. 1177-1180.

Eugster, H.P., and Surdam, R.C., 1973, Depositional Environment of the Green River Formation of Wyoming, A Preliminary Report: Geological Society America Bulletin, v. 84, no. 4, p. 1115-1120.

Feng, J., 2011, Source Rock Characterization of the Green River Oil Shale, Piceance Creek Basin, Colorado, MS Thesis, Colorado School of Mines, Golden, Colorado, 115p.

Fischer A.G., 1965, Fossils, Early Life, and Atmospheric History: Proceedings of the National Academy of Sciences of the United States of America, v. 53, p.1205–1215.

Frantz, C.M., Petryshyn, V.A., Marenco, P.J., Tripati, A., Berelson, W.M., and Corsetti, F.A., 2014, Dramatic Local Environmental Change during the Early Eocene Climatic Optimum Detected using High Resolution Chemical Analyses of Green River Formation Stromatolites: Palaeogeography, Palaeoclimatology, Palaeoecology, v. 405, p. 1-15.

Gallegos, E.J., 1973, Identification of Phenylcycloparaffin Alkanes and other Monoaromatics in Green River Shale by Gas Chromatography-Mass Spectroscopy: Analytical Chemistry, v. 45, no. 8, p. 1399-1403.

George, A., Lazar, S., and Booth, J., 2012, Mounds and Boundstone Facies in the Late Carboniferous-Early Permian Pha Nok Khao Formation-Equivalent of the Loei Syncline, Loei-Phetchabun Foldbelt: Implications for Reservoir Quality, paper presented at International Petroleum Technology Conference held in Thailand, February 7-9, p. 1–6.

Grantham, P.J., 1986, The Occurrence of Unusual C_{27} and C_{29} Sterane Predominances in Two Types of Oman Crude Oil: Organic Geochemistry, v. 9, no. 1, p. 1-10.

Grotzinger, J.P., and Knoll, A.H., 1995, Anomalous Carbonate Precipitates: Is the Precambrian the Key to the Permian?: Palaios, v. 10, p. 578-596.

Grotzinger, J.P., and Rothman, D.R., 1996, An Abiotic Model for Stromatolite Morphogenesis: Nature, v. 383, p. 423-425.

Grotzinger, J.P., Knoll, A.H., 1999, Stromatolites in Precambrian Carbonates: Evolutionary Mileposts or Environmental Dipsticks?: Annual Reviews of Earth and Planetary Sciences, v. 27, p. 313-358.

Al Haddad, S., and Mancini, E.A., 2013, Reservoir Characterization, Modeling, and Evaluation of Upper Jurassic Smackover Microbial Carbonate and Associated Facies in Little Cedar Creek Field, Southwest Alabama, Eastern Gulf Coastal Plain of the United States: AAPG Bulletin, v. 97, no. 11, p. 2059–2083.

Hamon, Y., Sebastien, R., Deschamps, R., and Gasparrini, M., 2012, Outcrop Analogue of Pre-Salt Microbial Series from South Atlantic: the Yacoraite Fm, Salta Rift System, paper presented at AAPG Hedberg Conference held in Houston, Texas, June 4-8, p. 1–4.

Hardie, L.A., and Eugster, H.P., 1970, The Evolution of Closed-Basin Brines: Mineralogical Society of America Special Publication, v. 3, p. 273-290.

Holba, A.G., Tegelaar, E., Ellis, L., Singletary, M.S., and Albrecht, P., 2000, Tetracyclic Polyprenoids: Indicators of Freshwater (lacustrine) Algal Input: Geology, v. 28, no. 3, p. 251–254.

Huang, W.Y., Meinschein, W.G., 1979, Sterols as Ecological Indicators: Geochimica et Cosmochimica Acta, v. 43, no. 5, p. 739-745.

Johnson, R.C., 1985, Early Cenozoic History of the Uinta and Piceance Creek Basins, Utah and Colorado, with Special Reference to the Development of Eocene Lake Uinta: Rocky Mountain Section, SEPM, p. 247-276.

Johnson, R.C., Mercier, T.J., Brownfield, M.E., Self, J.G., 2010, Assessment of In-place Oil Shale Resources of the Green River Formation, Uinta Basin, Utah and Colorado: U.S. Geological Survey Fact Sheet. p. 2010-3010.

Kalkowsky, E., 1908, Oolith und Stromatolith im Norddeutschen Buntsandstein. Zeitschrift Deutschen geol. Gesellschaft, v. 60, p. 68–125.

Kempe, S., Kazmierczak, J., Landmann, G., Konuk, T., Reimer, A., and Lipp, A., 1991, Largest Known Microbialites Discovered in Lake Van, Turkey: Nature, v. 349, p. 605-608.

Killops, S.D., and Killops, V.J., 2009, Introduction to Organic Geochemistry: Blackwell Science, 406 p.

Kopaska-Merkel, D.C., Mann, S.D., and Pashin, J.C., 2013, Sponge-Microbial Mound Facies in Mississippian Tuscumbia Limestone, Walker County, Alabama: AAPG Bulletin, v. 97, no. 11, p. 1871–1893.

Koralegadara, G., and Parcell, W.C., 2008, Reservoir Characterization of Microbial Reef Reservoirs at Little Cedar Creek Field, Conecuh County, Alabama, paper presented at 4th Annual Symposium on Graduate Research and Scholarly Projects held in Wichita, KS at Wichita State University, April 25, p. 57–58.

Lentini, M.R., Fraser, S.I., Sumner, H.S., and Davies, R.J., 2010, Geodynamics of the Central South Atlantic Conjugate Margins: Implications for Hydrocarbon Potential: Petroleum Geoscience, v. 16, no. 3, p. 217–229.

Lijmbach, G.W.M., 1975, On the Origin of Petroleum: Proceedings of the Worm Petroleum Congress, Special Paper, v. 1, p. 357-374.

Lindsay, J.F., Braiser, M.D., McLoughlin, N., Green, O.R., Fogel, M., McNamara, K., Steele, A., and Mertzman, S.A., 2003, Abiotic Earth-Establishing a Baseline for Earliest Life, Data from the Archean of Western Australia: Lunar and Planetary Institute, Annual Meeting, Lunar, Planetary Institute Contribution, v. 1156, p. 1137.

Lowe, D.R., 1994, Abiological Origin of Described Stromatolites Older than 3.2 Ga.: Geology, v. 22, no. 5, p. 387-390.

Mancini, E.A., and Parcell, W.C., 2001, Outcrop Analogs for Reservoir Characterization and Modeling of Smackover Microbial Reefs in the Northeastern Gulf of Mexico Area: Gulf Coast Association of Geological Societies Transactions, v. LI, p. 207–218.

Mancini, E.A., Parcell, W.C., Ahr, W.M., Ramirez, V.O., Llinás, J.C., and Cameron, M., 2008, Upper Jurassic Updip Stratigraphic Trap and Associated Smackover Microbial and Nearshore Carbonate Facies, Eastern Gulf Coastal Plain: AAPG Bulletin, v. 92, no. 4, p. 417–442.

Moncure, G., and Surdam, R.C., 1980, Depositional Environment of the Green River Formation in the Vicinity of the Douglas Creek Arch, Colorado and Utah: Contributions to Geology, v. 19, no. 1, p. 9–24.

Mueller, E., 1998, Temporal and Spatial Source Rock Variations and the Consequence on Crude Oil Compositions in the Tertiary Petroleum System of the Uinta Basin, Utah, U. S.A. Ph.D dissertation, University of Oklahoma, 170 p.

Noffke, N., Awramik, S.M., 2013, Stromatolites and MISS—Differences between Relatives: Geological Society of America Today, v. 23, p. 4–9.

Nombo-Makaya, N.L., Hong Han, C., 2009, Pre-Salt Petroleum System of Vandji-Conkouati Structure (Lower Congo Basin), Republic of Congo: Research Journal of Applied Sciences, v. 4, no. 3, p. 101-107.

Olcott, A.N., Sessions, A.L., Corsetti, F.A., Kaufman, A.J., De Oliviera, T.F., 2005, Biomarker Evidence for Photosynthesis During Neoproterozoic Glaciation: Science, v. 310, p. 471–474.

Osburn, M., Grotzinger, J., and Bergmann, K., 2013, Facies, Stratigraphy, and Evolution of a Middle Ediacaran Carbonate Ramp: Khufai Formation, Sultanate of Oman: AAPG Bulletin, v. 98, no. 8, p. 1631-1667.

Osmond, J.C., Willow, W., and Field, C., 2000, West Willow Creek Field: First Productive Lacustrine Stromatolite Mound in the Eocene Green River Formation, Uinta Basin, Utah: The Mountain Geologist, v. 37, no. 3, p. 157-170.

Ourisson, G., Albrecht, P., and Rohmer, M., 1982, Predictive Microbial Biochemistry, a Forensic Approach to Prokaryotic Membrane Constituents: Trends Biochemistry Science, v. 7, p. 236–239.

Pacton, M., Gorin, G.E., Vasconcelos, C., 2011, Amorphous Organic Matter - Experimental Data on Formation and the Role of Microbes: Review of Palaeobotany and Palynology, v. 166, p. 253-267.

Parcell, W.C., 2002, Sequence Stratigraphic Controls on the Development of Microbial Fabrics and Growth Forms - Implications For Reservoir Quality Distribution In The Upper Jurassic (Oxfordian) Smackover Formation, Eastern Gulf Coast, USA: Carbonates and Evaporites, v. 17, p. 166-181.

Patterson, G.W., 1977, The Distribution of Sterols in Algae: Lipids, v. 6, no. 1, p. 20-27

Peters, K.E., 1986, Guidelines for Evaluating Petroleum Source Rock using Programmed Pyrolysis, AAPG Bulletin, v. 70, no. 3, p. 318-329.

Peters, K.E., and M.R., Cassa, 1994, Applied Source Rock Geochemistry, *in* The Petroleum System--From Source Rock to Trap, Edited by Magoon, L.B., and W.G., Dow: AAPG Memoir, v. 60, p. 93-120.

Peters, K.E., Walters, C.C., and Moldowan, J.M., 2005a, The Biomarker Guide: Volume 1, Biomarkers and Isotopes in the Environment and Human History, Cambridge University Press, 471 p.

Peters, K.E., Walters, C.C., and Moldowan, J.M., 2005b, The Biomarker Guide: Volume 2, Biomarkers and Isotopes in the Environment and Earth History, Cambridge University Press, 1107 p.

Pitman, J.K., 1996, Origin of Primary and Diagenetic Carbonates in the Lacustrine Green River Formation (Eocene), Colorado and Utah: U.S. Geological Survey Bulletin, p. 21-57.

Platt, N.H., and Wright, V.P., (1991) Lacustrine Carbonates: Facies Models, Facies Distributions and Hydrocarbon Aspects, in Lacustrine Facies Analysis, Edited by Anadón, P., Cabrera, L.I., and Kelts, K., Blackwell Publishing Ltd., Oxford, UK, p. 57-74.

Powell, T.G., and McKirdy, D.M., 1973, Relationship between Ratio of Pristane to Phytane, Crude Oil Composition and Geological Environment in Australia: Nature, v. 243, p. 37-39.

Price, L.C., 1993, Thermal Stability of Hydrocarbons in Nature: Limits, Evidence, Characteristics, and Possible Controls: Geochimica et. Cosmochimica Acta, v. 57, p. 3261–3280.

Riding, R., 2000, Microbial Carbonates: The Geological Record of Calcified Bacterial–Algal Mats and Biofilms: Sedimentology, v. 47, p. 179–214.

Riding, R., 2006, Cyanobacterial Calcification, Carbon Dioxide Concentrating Mechanisms, and Proterozoic-Cambrian Changes in Atmospheric Composition: Geobiology, v. 4, p. 299-316.

Riding, R., 2010, The Nature of Stromatolites: 3,500 Million Years of History and a Century of Research, *in* Advances in Stromatolite Geobiology, Edited by Reitner, J., Trauth, M.H., Stuwe, K., and Yuen, D., Lecture Notes in Earth Sciences, v. 131, Springer Berlin Heidelberg, p. 29–74.

Riding, R., 2011, Microbialites, Stromatolites, and Thrombolites, *in* Encyclopedia of Geobiology, Edited by Reitner, J., and Thiel, V., Springer Berlin Heidelberg, p. 635–654.

Roehler, H.W., 1974, Depositional Environments of Rocks in the Piceance Creek Basin, Colorado, *in* Guidebook to the Energy Resources of the Piceance Creek Basin, Colorado, Rocky Mountain Association of Geologists, 25th Annual Field Conference, Edited by Murray, D.K., p. 57-69.

Rohmer, M., Bouvier-Nave, P., and Ourisson, G., 1984, Distribution of Hopanoid Triterpenes in Prokaryotes: Journal of General Microbiology, v. 130, p. 1137–1150.

Sanei, H., Stasiuk, L.D., Goodarzi, F., 2005, Petrological Changes Occurring in Organic Matter from Recent Lacustrine Sediments during Thermal Alteration by Rock-Eval Pyrolosis: Organic Geochemistry, v. 36, p. 1190-1203.

Sarg, J.F., Suriamin, N., Tanavsuu-Milkeviciene, K., and Humphrey, J.D., 2013, Lithofacies, Stable Isotopic Composition, and Stratigraphic Evolution of Microbial and Associated Carbonates, Green River Formation (Eocene), Piceance Basin, Colorado: AAPG Bulletin, v. 97, no. 11, p. 1937–1966.

Schiefelbein, C.F., Zumberge, J.E., Cameron, N.R., and Brown, S.W., 1999, Petroleum Systems in the South Atlantic Margins: Geological Society, London, Special Publications, v. 153, no. 1. p. 169-179.

Schnurrenberger, D., Russell, J., and Kelts, K., 2003, Classification of Lacustrine Sediments Based on Sedimentary Components: Journal of Paleolimnology, v. 29, no. 2, p. 141-154.

Seard, C., Camoin, G., Rouchy, J.M., and Virgone, A., 2013, Composition, Structure and Evolution of a Lacustrine Carbonate Margin Dominated by Microbialites: Case study from the Green River formation: Paleogeography, Paleoclimatology, Paleoecology, v. 381-382, p. 128–144.

Sewall, J.O., and Sloan, L.C., 2006, Come a Little Bit Closer: A High-Resolution Climate Study of the Early Paleogene Laramide Foreland: Geology, v. 34, p. 81–84.

Siljeström, S., Lausmaa, J., Sjövall, P., Broman, C., Thiel, V., and Hode, T., 2010, Analysis of Hopanes and Steranes in Single Oil-Bearing Fluid Inclusions using Time-of-Flight Secondary Ion Mass Spectrometry (ToF-SIMS): Geobiology, v. 8, no. 1, p. 37–44.

Sinninghe Damsté, J.S., Kenig, F., Koopmans, M.P., Köster, J., Schouten, S., Hates, J.M. and de Leeuw, J.W., 1995, Evidence for Gammacerane as an Indicator of Water Column Stratification: Geochimica et. Cosmochimica Acta, v. 59, no. 9, p. 1895-1900.

Slowakiewicz, M., Tucker, M.E., Pancost, R.D., Perri, E., and Mawson, M., 2013, Upper Permian (Zechstein) Microbialites: Supratidal through Deep Subtidal Deposition, Source Rock, and Reservoir Potential: AAPG Bulletin, v. 97, no. 11, p. 1921–1936.

Smith, J.W., 1980, Oil Shale Resources of the United States: Mineral Energy Resources, v. 23, no. 6, p. 1-20.

Sullivan, R., 1985, Origin of Lacustrine Rocks of Wilkins Peak Member, Wyoming: AAPG Bulletin, v. 69, no. 6, p. 913-922.

Surdam, RC, Wolfbauer, C.A., 1975, Green River Formation, Wyoming: A Playa-Lake Complex: Geological Society of America, v. 86, no. 3, p. 335-345.

Talbot, H.M., Watson, D.F., Pearson, E.J., and Farrimond, P., 2003, Diverse Biohopanoid Compositions of Non-marine Sediments: Organic Geochemistry, v. 34, p. 1353–1371.

Tänavsuu-Milkeviciene, K.A., and Sarg, J.F., 2012, Evolution of an Organic-Rich Lake Basin Strtaigraphy, Climate, and Tectonics: Piceance Creek Basin, Eocene Green River Formation: Sedimentolog, v. 59, no. 6, p. 1735-1768.

ten Haven, H.L., Rohmer, M., Rullkotter, J., and Bisseret, P., 1989, Tetrahymanol, the Most likely Precursor of Gammacerane, Occurs Ubiquitously in Marine Sediments: Geochimica et. Cosmochimica Acta, v. 53, no. 11, p. 3073-3079.

Tissot, B., Deroo, G., and Hood, A., 1978, Geochemical Study of the Uinta Basin: Formation of Petroleum from the Green River Formation: Geochimica et Cosmochimica Acta, v. 42, no. 10, p. 1469-1485.

Trindade, L.A.F., Dias, J.L., and Mello, M.R., 1995, Sedimentological and Geochemical Characterization of the Lagoa Feia Formation, Rift Phase of the Campos Basin, Brazil, *in* Petroleum Source Rocks, Edited by Katz, B.J., Springer Berlin Heidelberg, p. 149-165.

Tuttle, M.L., and Goldhaber, M.B., 1991, Sulfur Geochemistry and Isotopy of the Green River Formation, Wyoming, Utah, and Colorado, *in* Geochemical, Biogeochemical, and Sedimentological Studies of the Green River Formation, Wyoming, Utah, and Colorado, Edited by Tuttle, M.L., U.S. Geological Survey Bulletin, U.S. Geological Survey, Denver, p. BI-B20.

Virgone, A., 2013, Continental Carbonates Reservoirs: The Importance of Analogues to Understand Presalt Discoveries, paper presented at the International Petroleum Technology Conference held in Beijing, China, March 26-28, p. 1–9.

Volkman, J.K., 2003, Sterols in Microorganisms: Applied Microbiology and Biotechnology, v. 60, no. 5, p. 495-506.

Volkman, J.K., 2005, Sterols and other Triterpenoids: Source Specificity and Evolution of Biosynthetic Pathways: Organic Geochemistry, v. 36, p. 139–159.

Wahlman, G.P., Orchard, D.M., and Buijs, G.J., 2013, Calcisponge-Microbialite Reef Facies, Middle Permian (Lower Guadalupian), Northwest Shelf Margin of Permian Basin, New Mexico: AAPG Bulletin, v. 97, no. 11, p. 1895–1919.

Wakeham, S.G., Schaffner, C., Giger, W., 1980, Polycyclic Aromatic Hydrocarbons in Recent Lake Sediments—I. Compounds having Anthropogenic Origins: Geochimica et Cosmochimica Acta, v. 44, no. 3, p. 403-413.

Walter, M.R., 1976, Stromatolites: Elsevier Science, 790 p.

Walters, C.C., Cassa, M.R., 1985, Regional Organic Geochemistry of Offshore Louisiana: Trans Gulf Coast Association of Geological Societies, v. 35, p. 277-86

Walter, M.R, Heys, G.R., 1985 Links between the Rise of the Metazoa and the Decline of Stromatolites: Precambrian Research, v. 29, p. 149-174.

Warusavitharana, C., and Parcell, W., 2013, Sedimentary Features, Occurrence, and Cyclicity of Microbialite Facies in the Roubidoux and Jefferson City Formations of Missouri and Kansas: AAPG Bulletin, v. 97, no. 11, p. 1849–1870.

Younes, M.A., and Philip, R.P., 2005, Petroleum Geochemistry and Potential Source Rock Correlation in the Shushan Basin, North Western Desert, Egypt: Petroleum Science and Technology, v. 23, no. 5-6, p. 507-536.

Young, R.G., 1995, Structural Controls Of The Piceance Creek Basin, Colorado, *in* The Green River Formation in Piceance Creek and Eastern Uinta Basins, Grand Junction Geological Society, Field Trip Guidebook, p. 23-29.